1.0

2.8 2.5

3.2 2.2

3.6

4.0 2.0

1.1

1.8

1.25 1.4 1.6

MICROCOPY RESOLUTION TEST CHART
NATIONAL BUREAU OF STANDARDS-1963-A

LEVEL II

(12)

(6)

PRELIMINARY STUDY OF A RECOIL MECHANISM USING COULOMB FRICTION

(10) C. Cusano, Project Director
H. J. Sommer, III, Research Assistant

Department of Mechanical and Industrial Engineering
University of Illinois at Urbana-Champaign
Urbana, IL 61801

(12) 78 p.

D D C
RECEIVED
SEP 25 1979
A

(11) July 79

79 08 20 078

400 833

TABLE OF CONTENTS

1. INTRODUCTION

This report is an initial study investigating the possible use of [illegible] for recoil energy dissipation in a friction recoil mechanism (FRM) for large bore cannon. Basic concepts and experimental friction material characteristics contributing to FRM functional and logistic feasibility are presented.

Hydro-pneumatic recoil mechanisms are currently used on large bore cannon to dissipate the kinetic energy of the recoiling mass by viscous [illegible] and to store a portion of that energy in a compressed gas to return the fully recoiled mass back to the firing position (counter-recoil). The intricate systems that have evolved over the years perform well but have logistic drawbacks due to seal failures and servicing complexity.

From practical considerations, a recoil mechanism should be a relatively passive system incorporating automatic or intrinsic actuation prior to or at firing, should be self-contained precluding external power sources, and should be tolerant of or compensate for variations in recoil travel. From a logistics standpoint, a recoil mechanism should demonstrate an extended in-service life, allow simple field servicing and repair, and permit long-term storage with rapid field recommission. The ultimate consideration of such a recoil system is its reliability over repeated firings. A single failure at any firing may cause catastrophic equipment damage and/or personnel injury.

Although current hydro-pneumatic recoil systems basically meet all of the above requirements, the comparative simplicity of conceptualized FRM hardware should allow superior performance in all three logistic areas stated above. FRM life/service interval would be a calculable function of the friction material wear rate and not a statistical estimate of effective seal life before failure. The simplicity and →next page

mechanical nature of FRM design should permit less complex service procedures. Simple separation of the friction rubbing interface and use of corrosive resistant friction/rubbing materials would facilitate long-term storage. Also, FRM operation will be insensitive to ambient temperature extremes, and the simplicity of hardware design should prove rugged and reliable enough to withstand any type of field transportation.

The main disadvantage of the FRM system is the effective application of the extremely high loads required for its actuation. In addition, a friction material would have to be selected which can withstand the severe operating conditions which exist in such a system. This study, therefore, will center about three primary considerations: friction pad loading methods, variation of coefficient of friction with temperature, load and speed, and the effects of surface contamination on the coefficient of friction. Basic concepts relative to the first topic and experimental friction results pertaining to the latter two topics are discussed in the following chapters.

As previously stated, simple and reliable mechanical means must be devised to generate extremely high normal forces for friction pad loading during recoil. The friction pads must be loaded before or at the instant of firing. Means must also be devised which will remove this actuating load at the end of recoil so that free FRM counter-recoil can take place.

While FRM friction materials must demonstrate good physical strength to withstand high normal and impulsive shear loads and resist edge shatter and scoring, the most important characteristic of these materials will be to maintain a moderate coefficient of friction with minimal variation with temperature, load, and speed. Excessive friction fade resulting from extended high temperature and high energy operation

will produce unacceptable recoil travel, and friction squeal/grab may cause lock-up of FRM systems with a high degree of self-energization.

Contamination (water, oil, dirt, etc.) of the friction interface will cut the coefficient of friction drastically and produce catastrophic FRM performance. Although limited friction recovery from small amounts of contamination may be expected, hardware design should attempt to prevent any contamination at all.

2. BASIC FRM ANALYTICAL CONCEPTS

The primary function of a recoil mechanism is to act as a shock absorber between the recoiling mass and the cannon mount by dissipating the sudden breech force impulse over a longer period of time. Traditionally, recoil mechanisms allow impulsive acceleration of the recoil mass, decelerate that mass over the length of recoil travel and also provide means for bringing the recoiling mass back to its firing position.

Frictional braking is commonly used in automotive, aircraft, and industrial applications to dissipate high kinetic energy levels by non-conservative frictional heat generation. An FRM would use this type of braking system during recoil* but would also require a secondary partially or totally conservative subsystem to store a portion of the recoil energy for counter-recoil.

To best determine the feasibility of an FRM, some very simple design concepts will be discussed. An FRM with a linear, as opposed to rotating, friction surface with constant or near constant friction pad loading is the basis for most of the following discussions.

Recoil Simulations--Equations for the recoil force and computer integration of recoil mass motion were used for various FRM simulation purposes. All required physical data and breech force curves for the cannon were supplied by U.S. Army Armament RADCOM, Dover, New Jersey.

Two equations expressing the frictional recoil force required to produce a desired recoil travel are given in APPENDIX A. Sample calculations for 105 mm and 155 mm cannon are also included. Both equations

---

*It should be noted that in normal frictional braking, the friction material is usually loaded against a moving surface. FRM braking will require friction material loading prior to any motion induced by firing which will cause impulsive friction interface shear loading at the instant of firing.

assume constant friction pad normal loading producing a constant frictional recoil force. The first equation is based on a simplifying assumption that the total breech force impulse occurs instantaneously at firing. The second equation is formulated more exactly using the actual impulse over time. The more exact equation corresponds accurately to computer simulations discussed later, while the total initial impulse concept produces reasonable but most importantly conservative predictions of required frictional force for given constraints.

It may be seen from these simple calculations that enormous normal forces and large pad areas must be used to generate sufficient FRM frictional forces. These equations clearly show that FRM frictional forces may be reduced for a larger recoil mass. These equations also show that travel is nearly inversely proportional to frictional force. This indicates that in a constant frictional force FRM, a 10 percent loss in friction will produce approximately a 10 percent increase in travel.

A computer program simulating recoil mass motion was written using Simpson time-integration of the forces acting on the recoil mass. The program was written to allow interactive user definition of various types and combinations of forces resisting recoil motion. This user definition of forces allowed simple simulation of various hybrid friction, spring, and viscous recoil mechanisms.

A listing and sample terminal session for the program are shown in APPENDIX B along with plots of three different simulations. The three simulations shown were all designed to produce a recoil travel of three feet for a 155 mm cannon although they used drastically different force functions to resist recoil motion.

Performances of two FRM frition pad loading methods (constant pad loading and a pad loading proportional to travel as generated by a recoil spring) are compared to a hypothetical hydro-pneumatic recoil mechanism performance. The primary recoil mechanism function of "spreading-out" the breech force impulse over time is also shown.

Based on these comparison plots, the hydro-pneumatic system demonstrates the most desirable energy dissipation performance. The hydro-pneumatic recoil force used was proportional to the square of the recoil velocity causing recoil energy dissipation at a rate proportional to the cube of that velocity. The constant load FRM can only dissipate energy at a rate proportional to the recoil velocity.

For equal travels, compared to a hydro-pneumatic system, a constant load FRM will develop higher maximum recoil speeds but will tend to distribute the generated heat more evenly along the friction rubbing track. Although the speed-time curves may differ, the change is negligible compared to projectile speed and should not have any appreciable effects on muzzle velocity and overall breech force impulse.

The same plot also demonstrates a very desirable trait of the constant load FRM. Because for constant friction load, the total energy dissipated is proportional to the product of the travel and the frictional force, a change in the coefficient of rubbing friction will result in an inversely proportional change in travel. The operation of a hydro-pneumatic system is much more sensitive to material (fluid) property variation.

The recoil spring loading FRM concept (with actuating force proportional to travel) shows poor energy dissipation and higher recoil speeds because the recoil force becomes maximum when the recoil speed is

a minimum and vice versa. This type of system is not recommended for recoil applications although a subsystem of this type could be used to provide for counter-recoil.

Friction Pad Loading--The energy which can be dissipated by a simple brake during recoil is a function of the activating force externally supplied to the brake. As shown previously, if caliper type brakes were used in an FRM, very large actuating forces would be needed to dissipate the recoil energy. Thus, for caliper-type brakes, it is not practical to apply an external force directly to the friction pads, but it is desirable to keep the external force as small as possible and to amplify this force, mechanically or otherwise, to obtain a large actuating force on the brake. This actuating force has to be applied before or at the instant recoil begins and also must be easily retractable at the end of recoil to allow for counter-recoil.

Hydraulic force application was not considered due to possible sealing problems similar to the current hydro-pneumatic recoil systems. An approach for applying the actuating force by using a centrifugal mechanism operated by the recoiling mass is probably not feasible because the time between the instant recoil begins and the time at which the centrifugal mechanism can effectively apply a force will be too long.

Two possible approaches for applying the activating force to the friction pads appear most feasible at this time. One of the approaches is to use a simple caliper-type brake system and apply the actuating force mechanically by means of a linear cam. The cam could be formed in the grounded or recoiling mass depending on whether the pads are attached to the grounded or recoiling mass. This technique converts recoil travel into follower travel which may be used to generate large

follower forces through the cam. To reduce the forces on the cam and follower, the force on the friction pad could be multiplied by a toggle-type mechanism which is actuated by the follower.

The second approach is to use self-energizing brakes. With this type of brake system, wedging action causes a normal force on the brake which increases nonlinearly with the coefficient of friction. With the self-energizing effect of the brake system, the required actuating force can be relatively small. The initial actuating force can be directly applied by using a cam or any other desired means.

Mechanical force amplifiers in the form of lever systems or toggles are one method which may be used to multiply actuation forces. A toggle unit is shown in APPENDIX C. Factors common to all linkage type force amplifiers may be seen in the toggle. These systems lend themselves well to FRM applications primarily through their simplicity of design.

Although mechanical systems such as levers and toggles may produce large force amplification by their large mechanical advantage (MA), they do not act as mechanical power amplifiers. This fact may cause adjust-ment problems produced by FRM friction pad wear. While the activating force at the pad is the product of the input force and the MA, any pad wear that takes place is reflected back at the input as the wear multi-plied by the MA. This may require considerable input force travel or mechanical in-service adjustments to compensate for friction pad wear.

In addition to the force amplification method described above, self-energizing friction pad loading methods may be used to further multiply effective pad actuation forces. In self-energizing systems, geometry of the pad loading is such that the frictional force itself is used to increase the effective pad normal force. Two such systems are

shown in APPENDIX C. One of the systems uses a frictional wedging
action while the other uses the moment created by the frictional force
on a pivoted pad to cause self-energization.

In the wedging concept, the frictional force and the actuation
force act together to wedge the pad against a ramp and produce a higher
effective pad normal force. This action can be described by a pad self-
energizing factor which is solely a function of geometry and the co-
efficient of friction of the friction pad. Self-actuation factors on
the order of 3 to 5 may be used for such systems by the proper selection
of the wedge angle. Wedging systems with larger self-actuation factors
are very friction sensitive and may become subject to frictional lock-up
(theoretically infinite self-actuation factor) with small increases in
the coefficient of friction of the pad.

A pivoted leading friction pad uses the moment of the friction
force about the offset pad pivot to augment the actuation force and
increase the effective pad normal force. The self-energizing factor for
this loading method is also solely a function of friction and geometry.
Self-energizing factors on the order of 1.5 to 3.0 may be used and are
limited functionally by practical geometry considerations. Although
lock-up is theoretically possible, the necessary geometry is functionally
impractical. Localized self-actuation of the pad trailing edge, how-
ever, may cause localized lock-up conditions and contribute to pad
trailing edge shatter.

Counter-Recoil--Irrespective of the FRM brake actuation method
used, it will be necessary to disengage the actuating force at the end
of recoil so that counter-recoil can take place. As the recoil ends, a
means must be provided to return the recoil mass to its initial position.

For simplicity, the energy required for counter-recoil should be stored during recoil. Various approaches were investigated for generating, storing and, subsequently, using this energy. By far, the simplest, most efficient, reliable, and compact approach studied was a mechanical spring.

Simple calculations show the maximum energy required for counter-recoil to be approximately 5 percent of the total recoil energy dissipated. Helical, compression springs are currently available which could handle both the travel and energy storage requirements for FRM counter-recoil and also provide rugged, reliable, long-term operation.

The required spring constant is a function of load to be raised (recoil mass), recoil distance, angle of cannon elevation, coefficient of friction between the recoiling and grounded masses, final velocity at end of counter-recoil and initial deflection of the spring. Using work-energy formulations, an expression relating the spring constant to the variables stated above was obtained as shown in APPENDIX D.

One of the most difficult counter-recoil variables to control is the recoil distance. If a constant brake actuating force were used, the recoil distance would vary with the effective coefficient of friction of the brake. The design of an FRM constant force recoil system would then have to be based on a minimum expected coefficient of friction because under this condition a maximum recoil travel would be expected. However, the design of an FRM counter-recoil spring would have to be based on a maximum expected coefficient of friction because for this condition a minimum recoil travel would be expected producing a minimum of stored spring energy.

This spring design criterion based on maximum expected friction is also demonstrated by the equation in APPENDIX D. Shorter recoil travels require larger spring constants for counter-recoil. This inverse variation of spring constant with recoil travel may be reduced by using larger preload deflections of the counter-recoil spring.

Frictional Heating--Frictional braking converts kinetic energy into thermal energy at the rubbing interface. This heat must be dissipated to prevent elevated temperatures in the friction and mating materials after multiple brake applications. Excessively high temperatures may cause fade of the coefficient of friction for the friction material and also may create surface failures (spalling, cracking, and oxidation) for both the friction and mating material.

For a metallic friction material on a steel mating material, over 90 percent of the frictional heat generated in braking will be conducted into the mating material [5]. Although FRM hardware design should allow some cooling of the friction pads, most of the cooling provided should dissipate heat from the friction ways. Direct convective heat transfer from the friction ways to the atmosphere is commonly used and should provide the simplest most effective means of cooling. Secondary heat exchangers using a fluid routed through cores in the friction ways may also be used but would greatly complicate way manufacture.

Because the heat of braking is generated at the friction surface, direct convective cooling at the rubbing surface of the friction ways should provide better heat dissipation than conduction of the heat through or along the friction ways to another convective surface. For this reason, external flat friction ways should provide cooler operation than comparable internal cylindrical friction ways without secondary coolant systems.

FRM braking using a constant friction force will not generate heat evenly along a linear friction way. The instantaneous heat flux per unit area into the friction way is proportional to the product of the pad loading normal pressure and the instantaneous recoil speed. Constant pad loading will generate heat at a linearly decreasing rate along the friction way. Added mass for thermal capacitance or additional cooling should then be provided at the fore end of the friction way to help create a more uniform temperature distribution along the way.

Numerical finite-difference conduction heat transfer simulations with convective surface losses have been successfully performed and validated for automotive and aircraft braking similar to FRM applications. However, such heat transfer calculations of frictional heating and convective cooling over multiple brake applications are extremely geometry dependent. Tentative conceptual hardware selections should be made (flat versus cylindrical ways, friction pad loading methods, counter-recoil system placement, etc.) before meaningful FRM temperature predictions can be accurately formulated using this method.

3. FRICTION MATERIALS TESTING

Overview--The primary purpose of the experimental portion of this project was to perform preliminary evaluations of various friction material types contemplated for use in a Coulomb friction recoil mechanism. In order to withstand the high impact and energy levels projected for an FRM, seven composite sintered metal friction materials were selected as possible candidates along with two steel mating materials. To investigate the effects of possible contaminants on the coefficient of friction of these materials, four projected brake surface contaminants were also studied. Constant speed drag tests were used for screening the friction materials. An over-arm milling machine was modified to rotate a heated, instrumented disc upon which a friction pad could be loaded as shown in Fig. 1.

The bulk of the tests conducted measured the friction performance of the selected materials in various clean and contaminated states at nominally selected loading, rubbing speed, and temperature of 300 psi, 40 fps, and 900°F, respectively. Further tests were conducted to estimate effects of variation in contaminant amount, load, speed, and temperature about these nominal values.

In regard to FRM conceptualizations, some of the primary friction material performance factors analyzed were: coefficient of friction and its variation with speed, load, and temperature; thermal fade; contaminant recovery; and cursory wear. Data from this preliminary screening of various friction materials can be used to make decisions about the feasibility of an FRM. It should be understood that these data should only be used as guidelines for future friction material
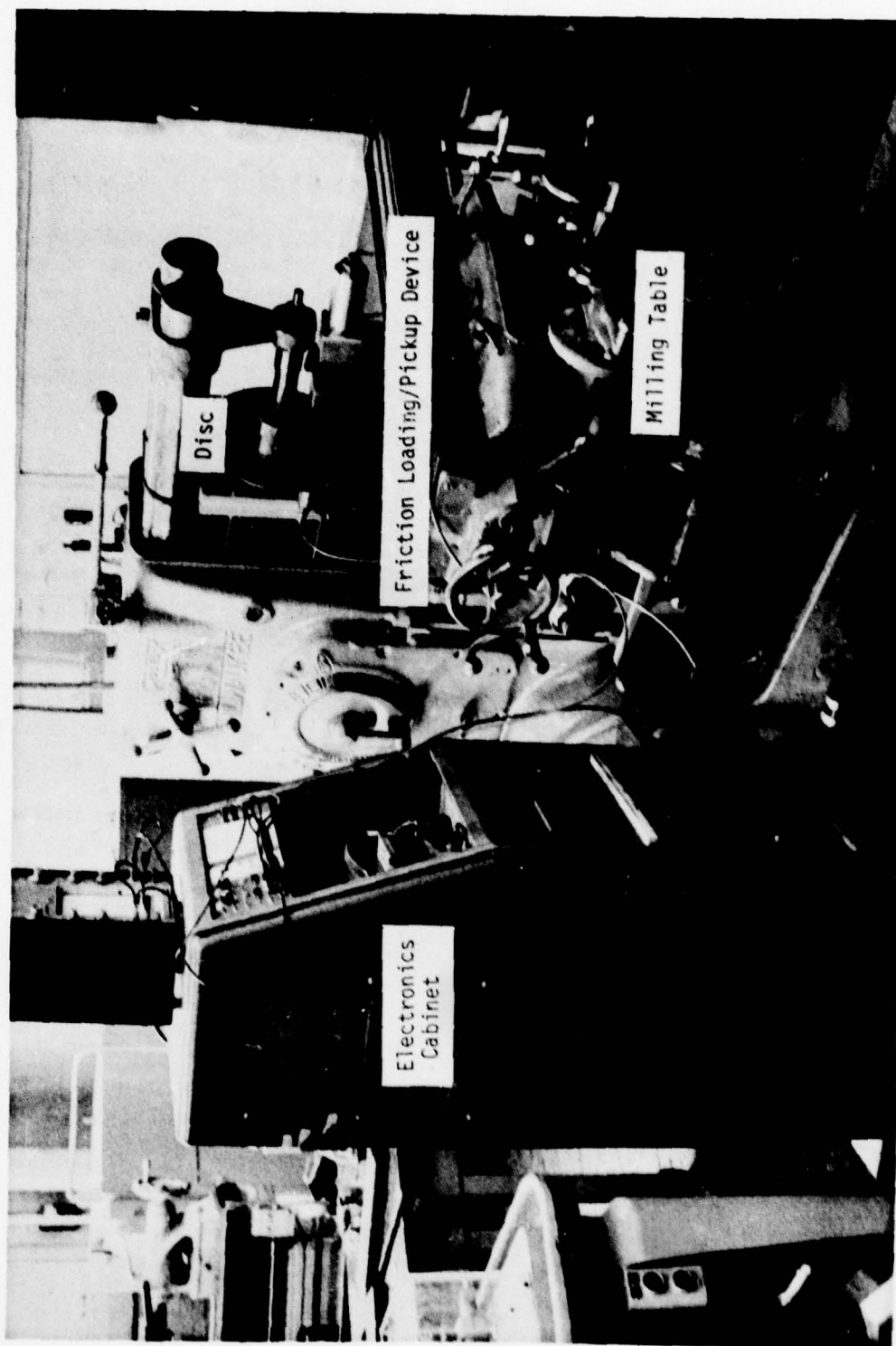
Figure 1 Friction Testing Apparatus

testing and as constraints for FRM conceptualizations. Exact friction material composition recommendations are beyond the scope of this study.

Materials--To promote cost effectiveness and reproducibility both for this project and future applications, commonly used and readily available materials were tested. The friction materials tested have either current or projected high energy braking applications in large off-road vehicles, commercial jumbo-jets, or fighter aircraft. The mating steels were common formulations and the contaminants were standard military lubricants or commercial products.

Candidate friction materials were selected which demonstrated a moderate to high coefficient of friction with minimal speed variation, thermal fade, and stick-slip conditions. Physically, the candidate materials were required to withstand high normal pressures, possess good shear impact strength, resist edge shatter from impulse loading, and demonstrate reasonable wear.

Because powdered metal friction materials generally conform to the above criteria, seven sintered metals (one copper base, three iron base, and three experimental nickel base) were selected for testing. Identification symbols used for these materials and other pertinent information are given in Table 1.

Sintered metal friction materials commonly have three primary components. These components are: base or binder metals, solid lubricants, and wear modifiers. The lubricant (traditionally graphite) reduces the base friction to help prevent localized seizing and overall grab and squeal. The wear modifier (traditionally a ceramic material) reduces wear and material transfer. Optimal constituent mixing for a specific application is very empirical and often held confidential by the friction materials industry.

Table 1 Sintered Metal Friction Materials Tested

Material	Base	Lubricant	Modified	Supplier	Supplier Designation
C1	Cu	Graphite	Mullite	Bendix	C60-43B
F1	Fe	Graphite	Mullite	ABEX	X-4511-L
F2	Fe	Graphite	Mullite	Friction Products	A-4B-11
F3	Fe	Graphite	Mullite	Friction Products	I-257-42B-42
N1	Ni	Graphite	--	NASA Lewis	Ni-30Gr
N2	Ni	Graphite	--	NASA Lewis	Ni-50Gr
N3	Ni	Rare Earth Oxide-Fluoride	--	NASA Lewis	$Ni-15La_2O_3$ $-15La\ F_3$

The friction material samples used were requested in the most convenient form from the suppliers to reduce sample lead time and greatly reduce sample expense by precluding the manufacture of special molds. Because many of the specimens could not be used in the shapes received, they had to be machined before they were tested. The hard, abrasive nature of the materials required machining at extremely slow material removal rates. However, prototype or production friction materials of this type may be easily and directly sintered into any desired form.

Because the mating material rubbing against the friction material must have extremely good physical strength and resist wear and corrosion, 17-22AS steel was one of the mating materials used in this study. The 17-22AS steel (0.3, 1.3Cr, 0.5Mo, 0.25V) is commonly used in aircraft brake discs. In addition, 4140 steel was used as a mating material because of its wide applications.

The 17-22AS steel is preferred in high-energy braking applications for its higher annealing temperature, surface finish retention, and wear resitance. To this end, a 17-22AS steel disc was tested as commonly used on aircraft brakes (Rc 48 hardness) and two, 4140 steel discs were tested (Rc 21 and Rc 50) to look at annealing, wear, and material transfer characteristics in the nominal thermal and load ranges expected in service.

Contamination of the friction rubbing interface by any of several media could greatly affect coefficient of friction and produce catastrophic FRM performance. Four possible contaminants (water, hydraulic fluid, grease, and grit) were selected for testing purposes. De-ionized water, hydraulic fluid MIL-H-6083C, and grease MIL-G-10942C were

introduced directly onto the friction interface to simulate possible field contaminations. The friction interface was bathed in a sand medium (AFS No. 125) to simulate a fine grit contamination.

Corrosion of both friction and mating materials could be another field contamination problem (especially for iron base materials). However, this contaminant was not simulated as it may be reasonably controlled chemically and/or logistically.

Apparatus--The testing equipment constructed for this study was designed for accurate, reliable friction material screening and cost effectiveness using existing hardware. An over-arm milling machine was used as the base of the friction testing apparatus. The machine table was used to mount the friction measurement equipment and to engage the friction material specimen against a mating material steel disc rotated at constant speed by the milling machine shaft as shown in Fig. 2.

The steel discs used (12 in. diamter by 0.5 in. thickness) accommodated four friction rubbing tracks (3.7, 4.3, 4.9, and 5.5 in. radii) per side. One disc (4140 Rc 50) was also instrumented with four thermocouples located axially 0.25 in. below the friction surface and radially beneath the centers of the rubbing tracks. Surface rubbing thermocouples were also used to approximately monitor disc rubbing track temperatures.

A special arbor and drawbar were constructed to allow passage of the thermocouple wires to the back of the machine where a slip ring and speed photo-pickup were mounted. An electric heating element was over-arm mounted to augment disc frictional heating.

Friction material specimen buttons (0.5 in. diameter by 0.2 to 0.3 in. thick) were clamped to a table-mounted, pre-loaded spring
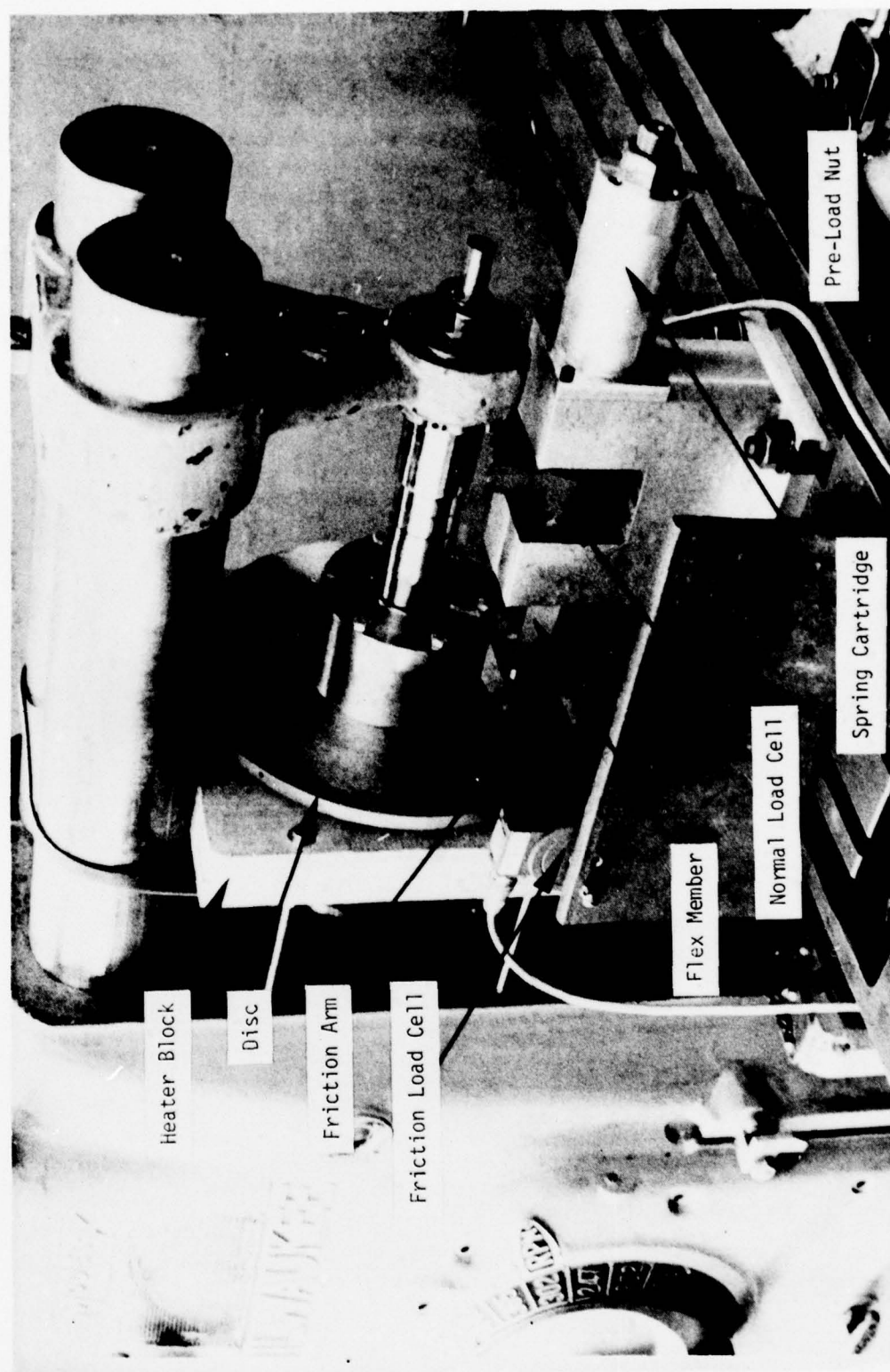
19

Figure 2 Friction Loading/Pickup Device (in position)

to provide constant load pad engagement by manually advancing the milling machine table as shown in Fig. 3. An in-line load cell measured the normal load of the pad. A flexure section was integral in the pad loading system to allow more sensitive friction force pickup by a second load cell after appropriate calibration.

Figure 4 shows a separate electronics cabinet which contained the following: two channels of special in-house designed load cell excitation, amplification, and filtering; photo-pickup power and counter; thermocouple selector and digital monitor; two channel chart recorder; and disc heater power connections and transformer.

Procedures--This study used constant speed drag testing at the mean recoil speed of 40 fps. This speed was estimated from FRM preliminary analytical simulations for a 155 mm cannon (see APPENDIX B). The normal pressure level used was 300 psi which is a nominal recommended maximum for these materials. The nominal maximum temperature for sustained operation of 900°F was selected based on previous studies [1-4].

Friction material specimen buttons were carefully machined to size, surface finished on 600 grit wet polishing paper, and cleaned with trichloroethylene. Each specimen button was weighed immediately prior to testing. The steel discs were reground to 16 microinch RMS surface finish after the eight available tracks (four per side) had been used to obtain friction data. Before beginning a series of tests on a side of a disc, the disc surface was also cleaned with trichloroethylene. Each test of a particular friction/mating material used a new friction button and the four rubbing tracks of a single side of a clean, reground disc.
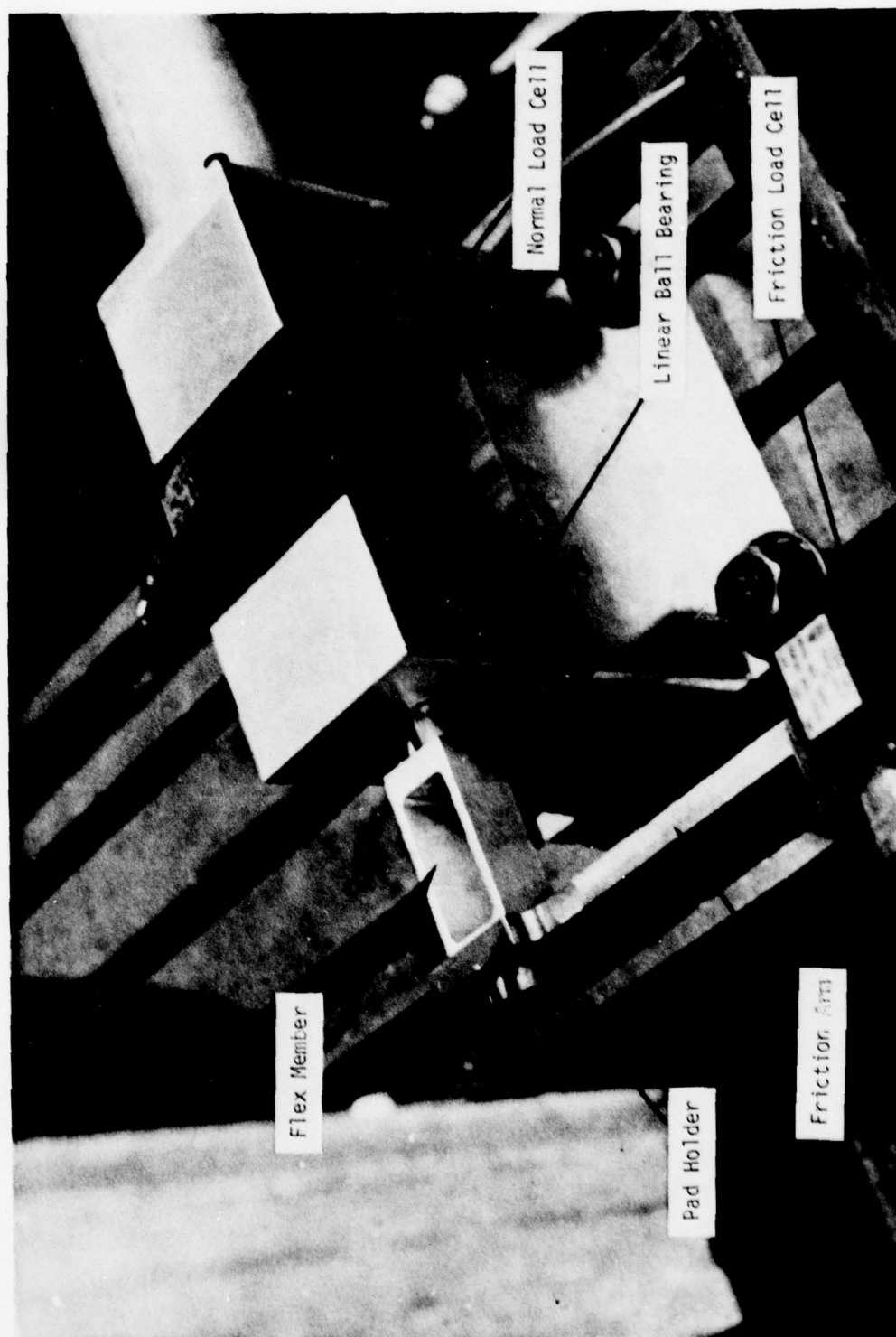
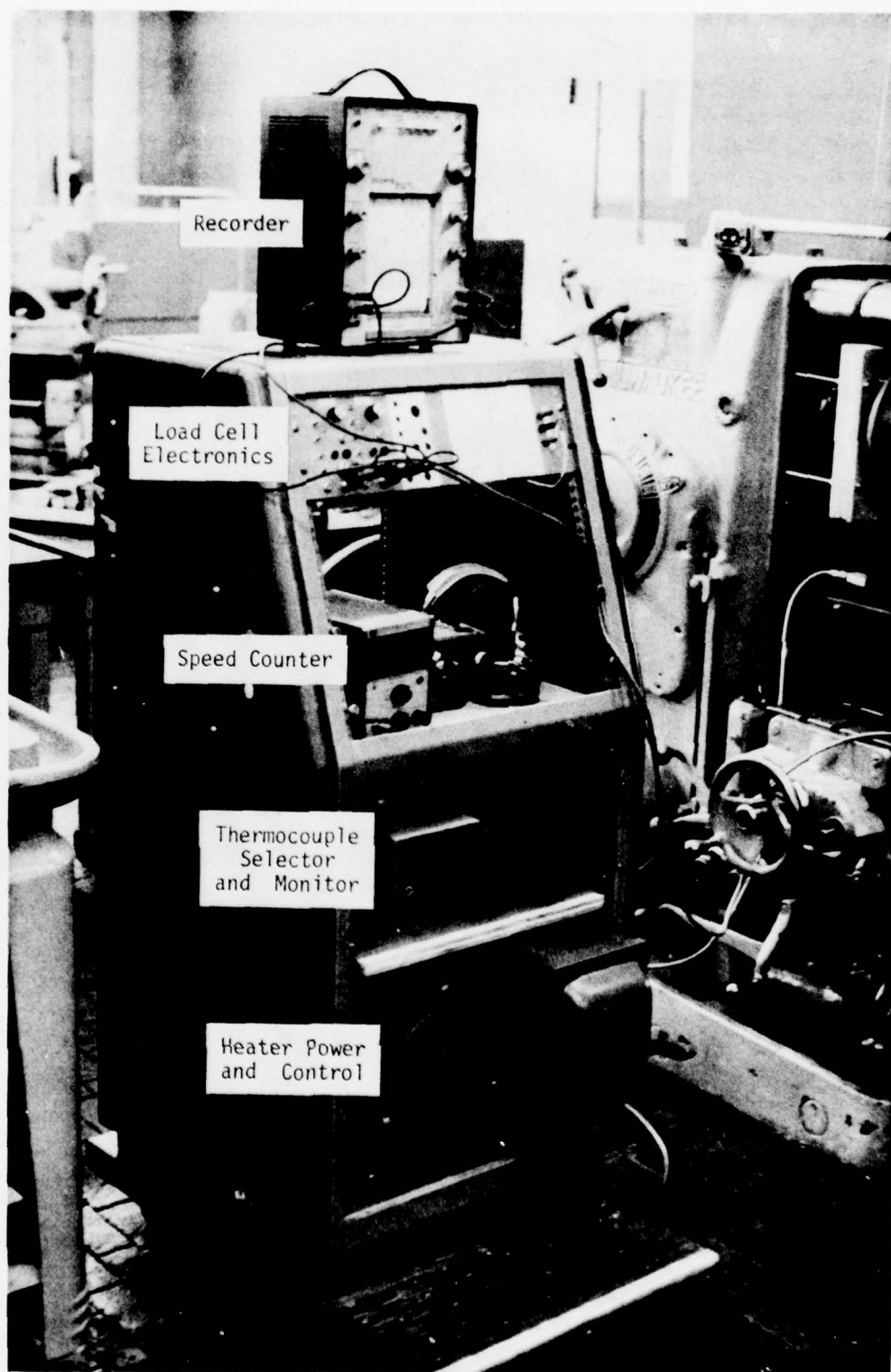Figure 3 Friction Loading/Pickup Device (withdrawn)

Figure 4 Electronics Cabinet

The basic testing sequence per disc side is defined as incorporating 28 separate friction runs of seven each on the four tracks. Outer to inner tracks were used successively. The seven runs on each track included three burnishing runs of 5 seconds duration each followed by four evaluation runs of 5, 10, 15, and 20 seconds duration, respectively. The seven runs on each track were separated by 5 seconds and the time from the end of the last run on one track to the initiation of the first run on the next track was approximately one minute.

The standard clean friction test of a friction/mating material pair is defined as using all four tracks of the above basic sequence with no friction interface contamination.

The standard contaminated friction test of a material pair is defined as the use of all four tracks on a side of the disc to investigate the effects of contaminants on the coefficient of friction. For these tests, the first track was used to obtain coefficient of friction data with no contaminants. Friction data under contaminated conditions were obtained by contaminating each of the remaining three tracks with either water, hydraulic fluid, or grease.* The basic track sequence above was used with contamination taking place immediately following the last burnish run on each track. The friction interface was contaminated by direct syringe injection of approximately 0.1 cc of contaminant with the disc rotating.

Grit contamination was simulated by dismounting the disc after the four track liquid contamination tests above were completed and agitating the disc in a fine sand bath. The disc was subsequently mounted and retested as above except without further burnishes or contaminations.

---

*Hereafter, these contaminants will be referred to as liquid contaminants.

The data recorded during any standard test (clean or contaminated) as described above included the following: mean coefficient of friction during each run and the variation thereof; the approximate maximum temperature (rubbing or bulk) experienced during each run; and friction pad weight loss after a complete test. In addition, visual observation of cursory wear and physical deterioration (scoring, edge shatter, crumbling, etc.) of the buttons and discs were noted.

Program--Complete contaminant tests (including sand contamination) were performed for the copper-base and all three iron-base friction materials against each of the three mating steel discs and for the three nickel friction materials against the 17-22AS steel disc giving 15 full contaminant tests in all. Two tests were repeated due to improper surface finish of the disc and another three tests were randomly chosen and repeated for validation checks.

In addition to the 15 standard contaminant tests above, several special tests were performed to measure how the coefficient of friction varied with four key parameters--contaminant, speed, pressure, and temperature. The special contaminant tests were subdivided into the following three areas: the investigation of friction material thermal fade versus contamination recovery, the effects of liquid recontamination after grit contamination on the coefficient of friction, and the effects on the coefficient of friction of the amount of grease on the track.

Contaminated friction tests do not generate temperatures on the rubbing surfaces as high as corresponding clean tests due to the reduction of coefficient of friction caused by contamination. Therefore, the coefficient of friction thermal fade should be more pronounced in clean tests than contaminated tests. Fade should also be more pronounced for the fourth track than for the first track in the basic

testing sequence due to accumulated frictional heat. To monitor fade
and help separate fade from contamination recovery for each rubbing
track, a standard clean friction test was performed using all four
rubbing racks of a disc side for each of two different friction/mating
material combinations.

A liquid and grit contamination test was peformed to demonstrate
simultaneously the effects of both of these contaminants on the coefficient
of friction. In this test, the disc was recontaminated with the liquid
contaminants after it was contaminated with grit.

To measure the effect of grease smear on friction recovery, seven
consecutive smear tests were performed on the same track of a disc after
three burnishes of five seconds duration each. The amount of smear
varied progressively from clean to the standard 0.1 cc smear in approxi-
mately equal steps of grease amount. After contamination, a minimum of
three evaluation runs of five seconds duration each were repeated with 5
second separations until the coefficient of friction had fully recovered.

Tests to determine the effects of varying temperature and pressure
on the coefficient of friction used a standard clean four track friction
test at nominal operating conditions as a baseline. Even though only
one track was needed for each of these tests, all four tracks on a side
of a disc were used in order to produce a more rigorous test from thermal
and energy standpoints.

Uncontaminated tests were repeated with the disc heater operating
at 50 and 100 percent capacity (approximately 1 and 2 kW, respectively)
for temperature variation studies. With the disc heater off, similar
tests were repeated using friction material normal pressures of 225 and
375 psi (representing 25 percent variation about the nominal 300 psi
value).

To investigate the coefficient of friction of the uncontaminated surfaces as a function of speed, consecutive runs (5 seconds duration with 15 seconds separation) were performed at nine rubbing speeds on the same disc track after three burnishes of five seconds duration each. The nine speeds varied from 4 fps to 64 fps.

Results--For clarity, the volume of experimental friction data generated has been condensed into 19 summary graphs. Because a single representative plot may concisely show similar effects evidenced by several or all friction/mating material combinations, only a small portion of the tests performed are plotted. The data represented may be grouped into eight categories as indicated in Table 2.

In all bar graph friction representations, the value plotted is the mean value recorded during the run. All friction values plotted as a central point and range represent the mean coefficient of friction and its variation during the run. Finally, all temperatures plotted are maximum disc bulk temperaures monitored during a run.

Summary--Overall, the friction material testing program produced very reproducible results which correlated well to previously published data and manufacturers supplied information. Although a limited set of friction materials was tested, many test parameter and contaminant effects on the coefficient of friction appear comparable for a wide range of friction material compositions.

One of the primary objectives of this program was to screen various friction materials for nominal uncontaminated coefficient of friction and friction variation for FRM design constraints. Table 3 details a summary of the basic performance of each of the friction materials tested.

Table 2 Guide to Plotted Friction Data

Category	Figure
1. Basic Clean and Liquid Contaminated Coefficients of Friction	5-11
2. Disc Material Effects	5,12, and 13
3. Fade Effects	5 and 14; 7 and 18
4. Grit Contamination Effects	5, 15, and 16
5. Grease Smear Amount Effects	5 and 17
6. Thermal Variation Effects	18, 19, and 20
7. Pressure Variation Effects	18, 21, and 22
8. Speed Variation Effects	18 and 23

28

Mean Coefficent of Friction

0.40 0.30 0.20 0.10 0.00

Track 1
Clean

0.36
0.36
0.35
0.36

Track 2
Water

0.09
0.34
0.35
0.35

Track 3
Hyd. Fl.

0.09
0.23
0.35
0.35

Track 4
Grease

0.08
0.21
0.26
0.34

5 10 15 20

Sequential Evaluation Runs (Duration in s)

Figure 5 C1 Friction Material on 17-22AS Disc
Standard Liquid Contaminants
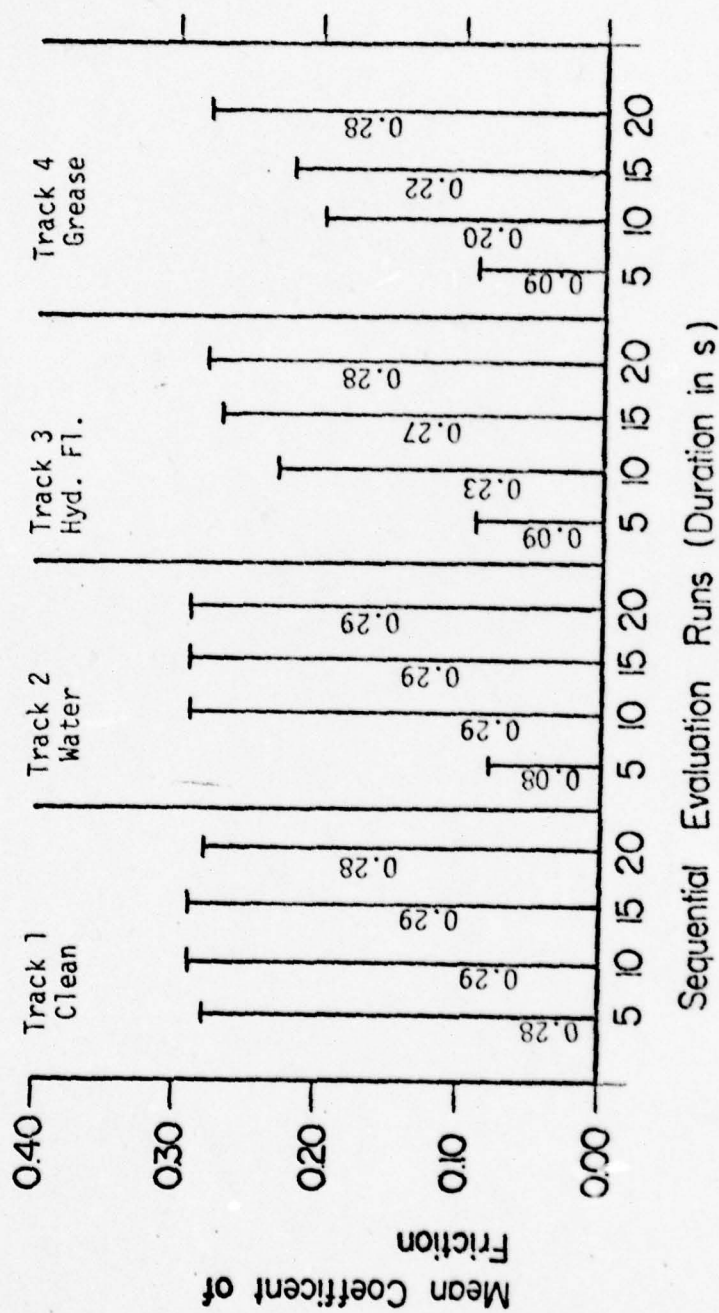
Figure 6 F1 Friction Material on 4140 Hard Disc
Standard Liquid Contaminants
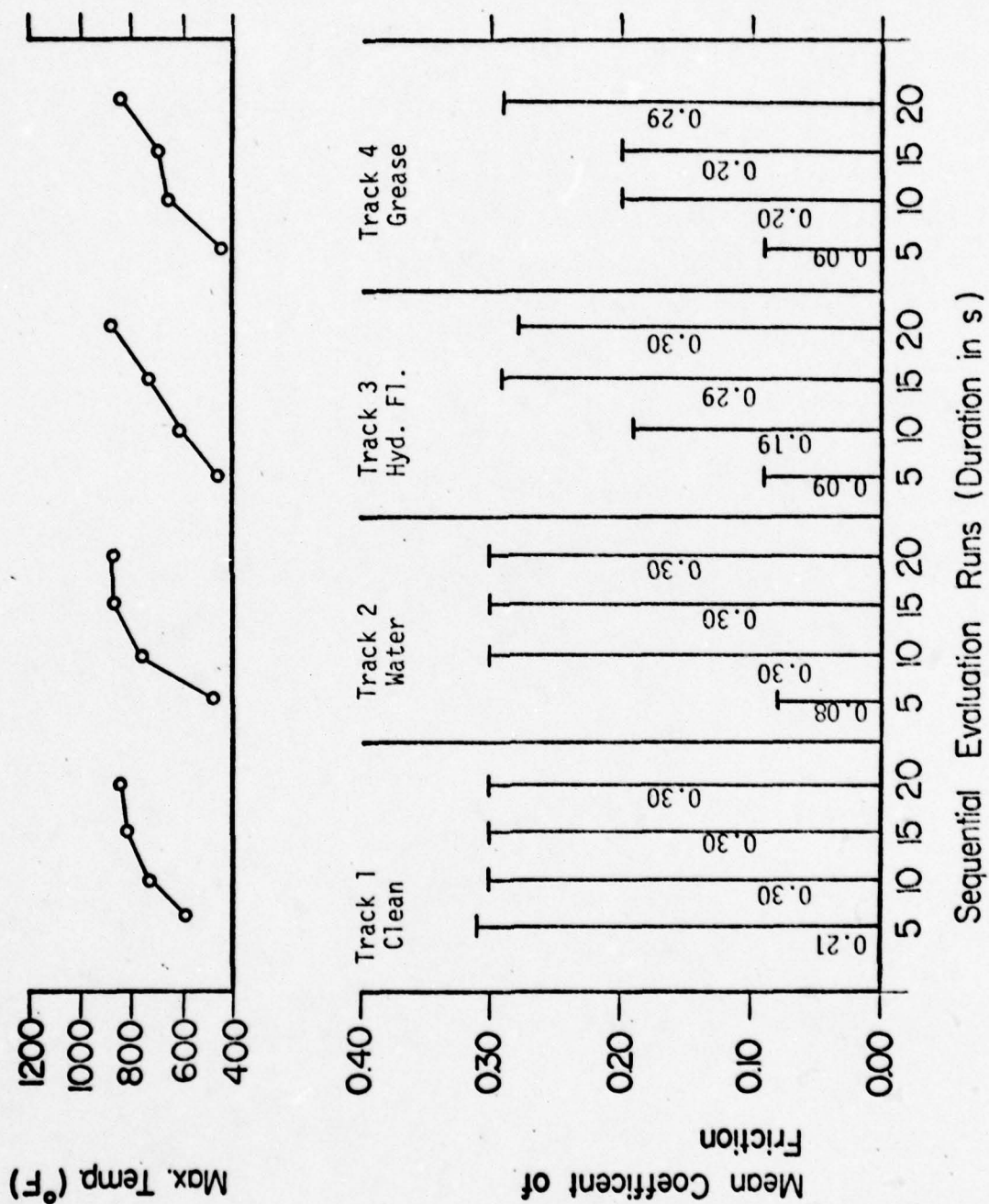
Figure 7 F2 Friction Material on 4140 Hard Disc
Standard Liquid Contaminants

Figure 8 F3 Friction Material on 4140 Hard Disc
Standard Liquid Contaminants
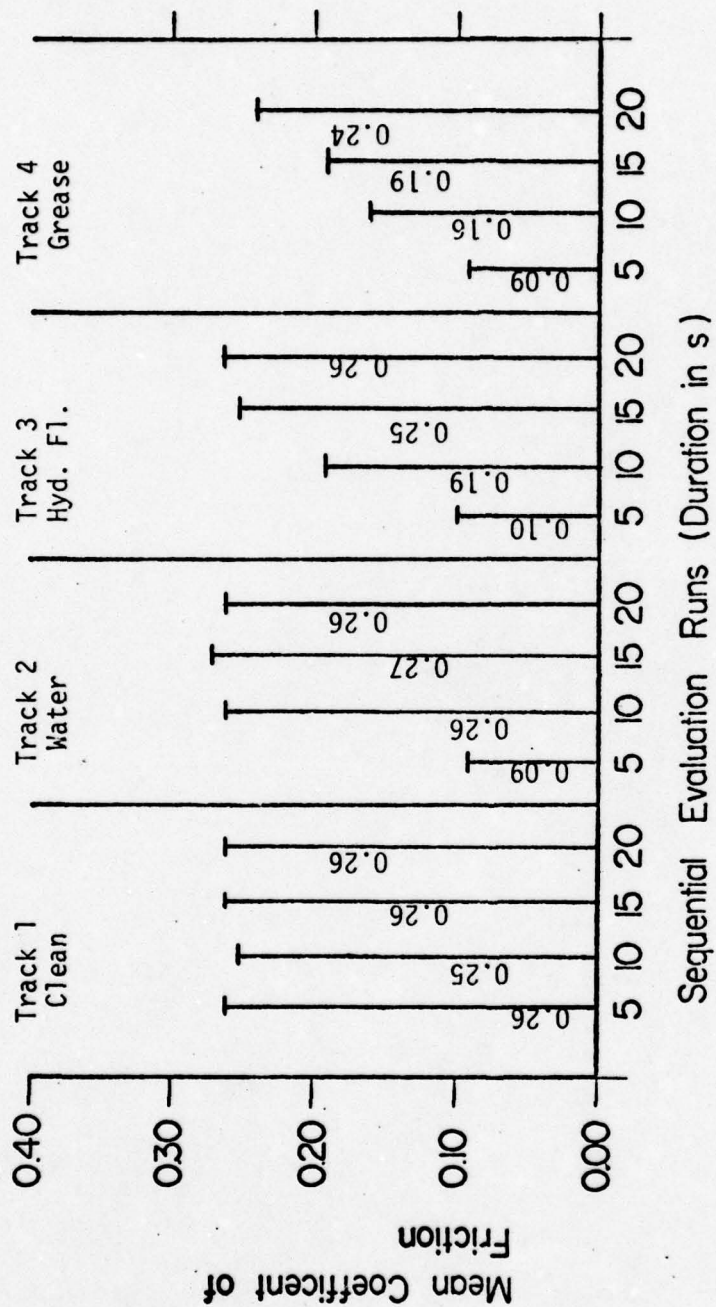
Figure 9   N1 Friction Material on 17-22AS Disc
Standard Liquid Contaminants
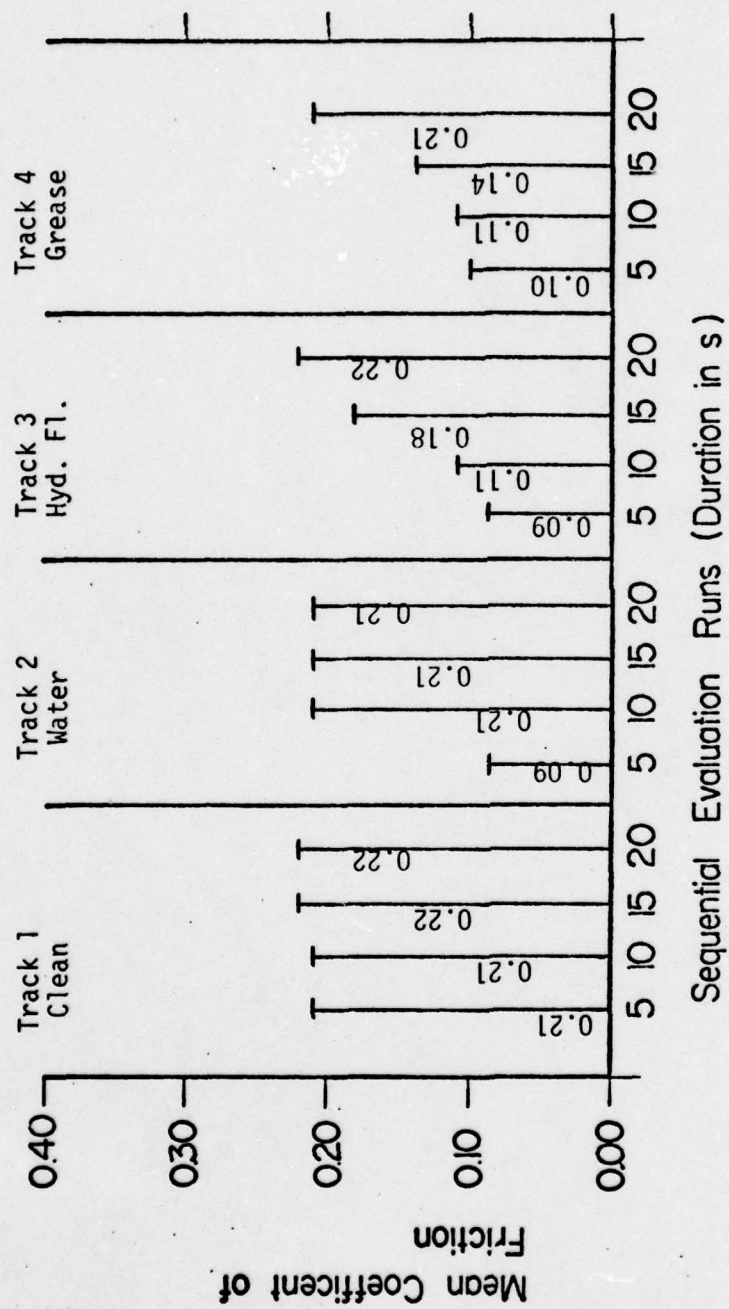
Figure 10 N2 Friction Material on 17-22AS Disc
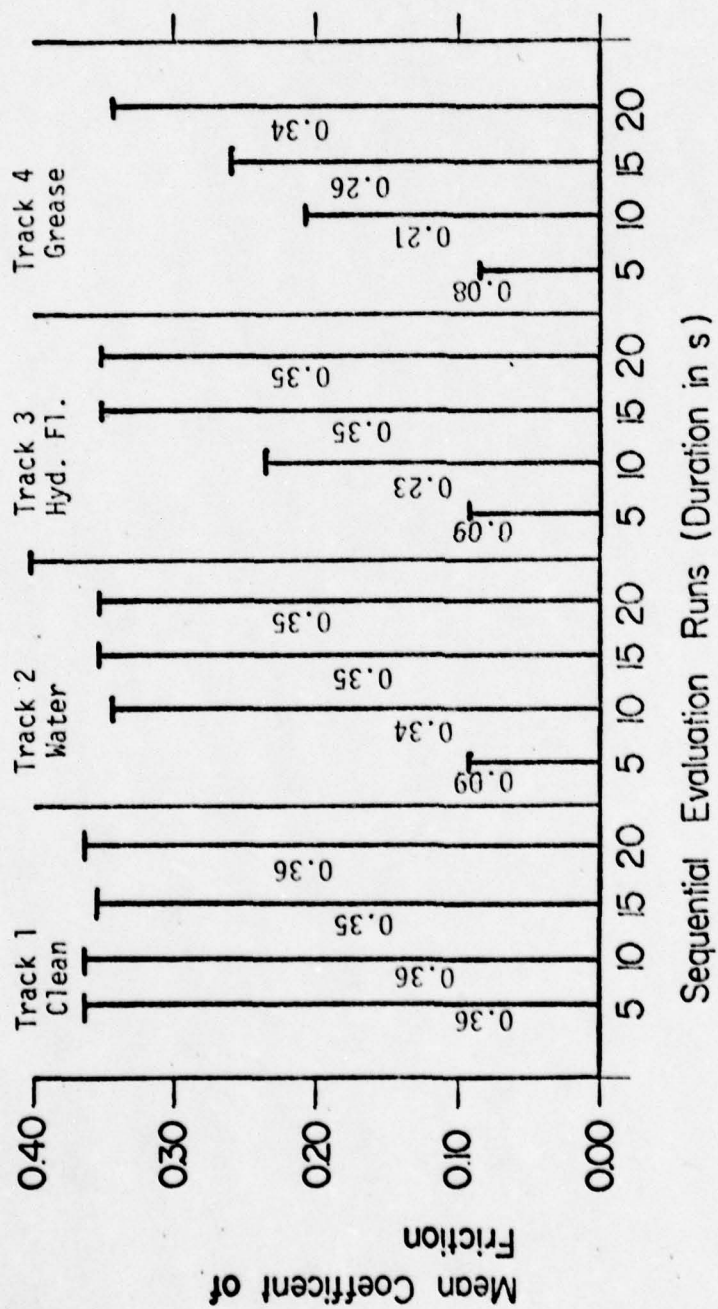Standard Liquid Contaminants

34
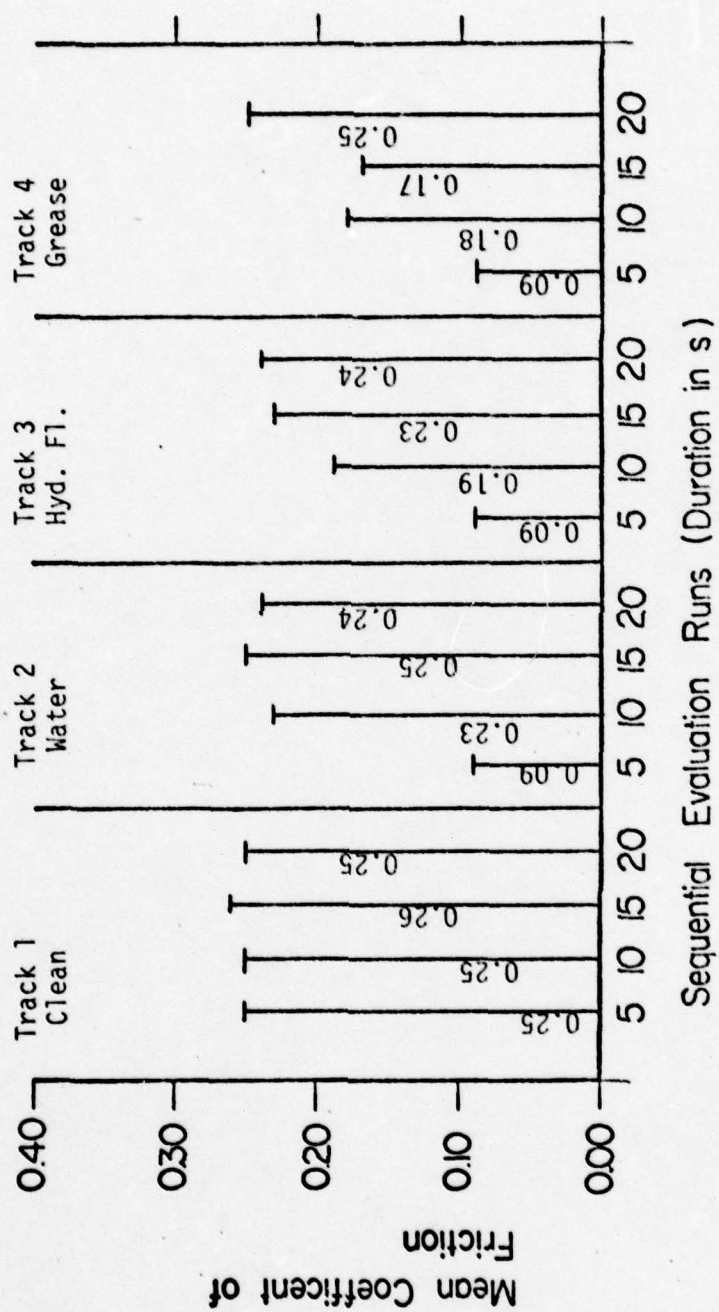
Figure 11 N3 Friction Material on 17-22AS Disc
Standard Liquid Contaminants
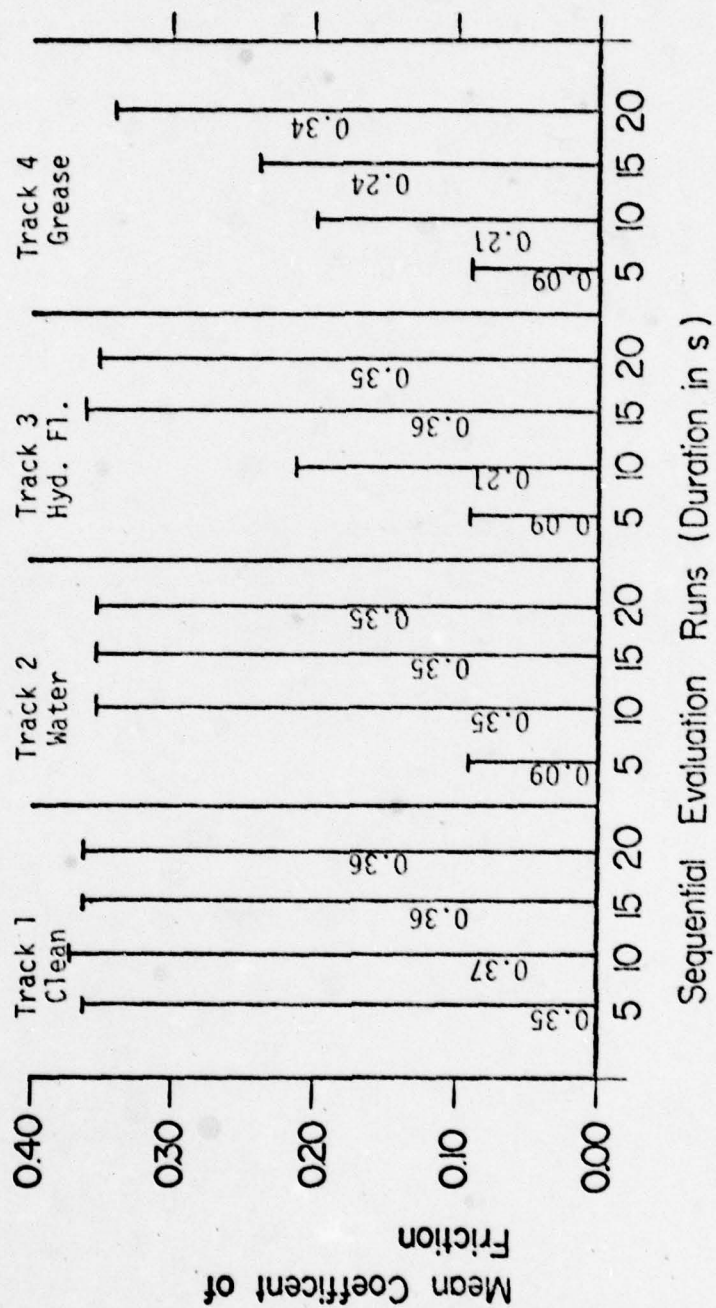
Figure 12 C1 Friction Material on 4140 Hard Disc
Standard Liquid Contaminants
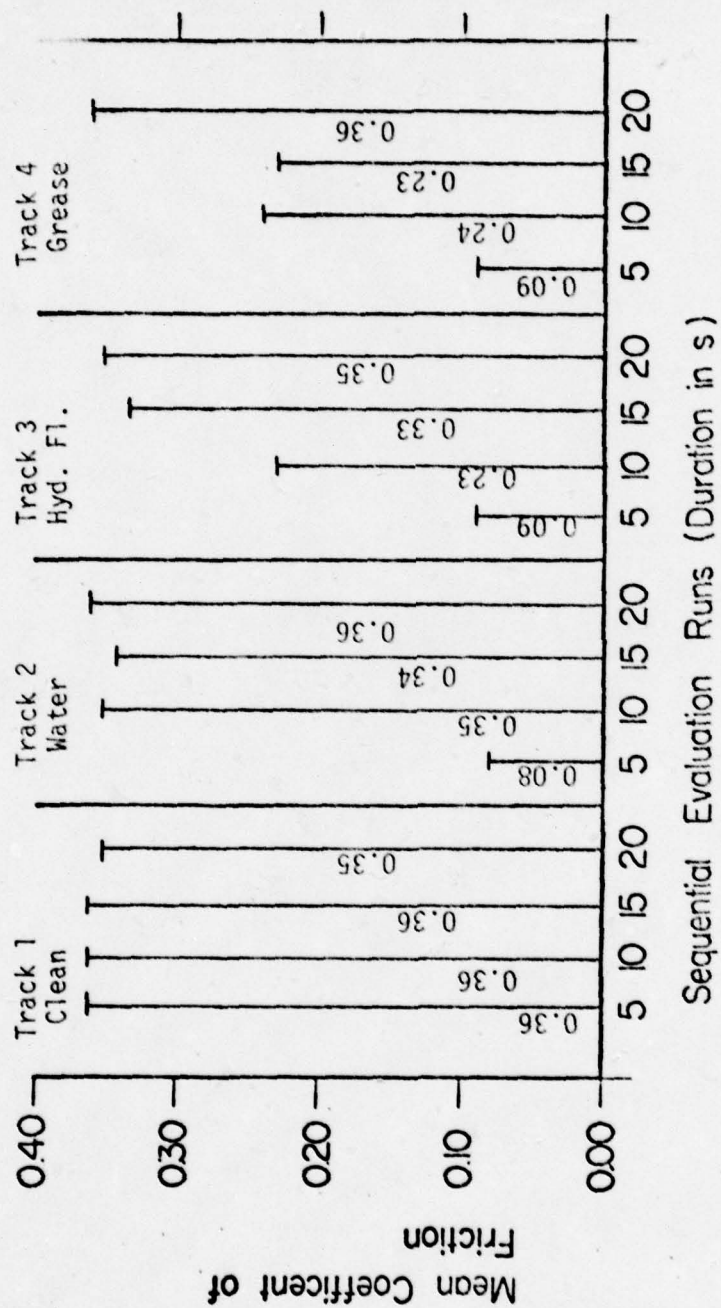
Figure 13 C1 Friction Material on 4140 Soft Disc
Standard Liquid Contaminants

Mean Coefficient of Friction

0.40

0.30

0.20

0.10

0.00

Track Clean

0.35 0.36 0.36 0.35

5 10 15 20

Track 2 Clean

0.35 0.36 0.37 0.36

5 10 15 20

Track 3 Clean

0.34 0.34 0.33 0.34

5 10 15 20

Track 4 Clean

0.31 0.33 0.32 0.33

5 10 15 20

Sequential Evaluation Runs (Duration in s)
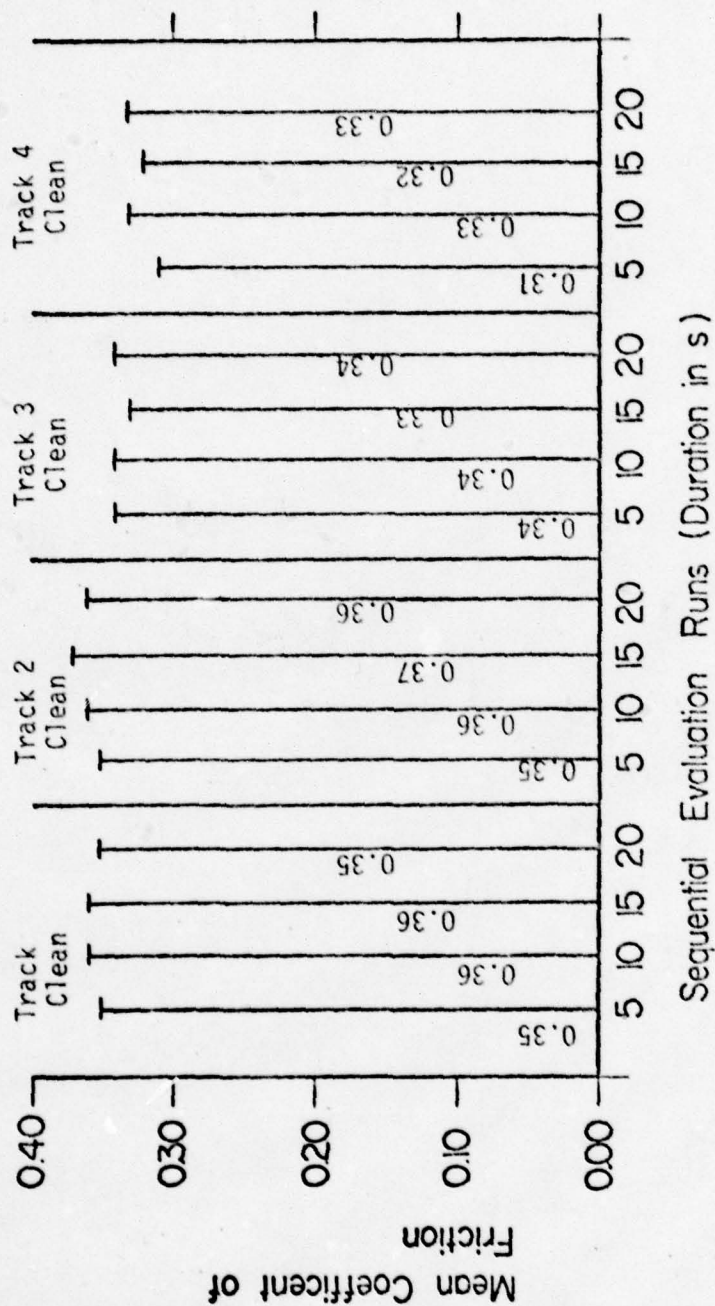
Figure 14 C1 Friction Material on 17-22AS Disc
No Contaminants
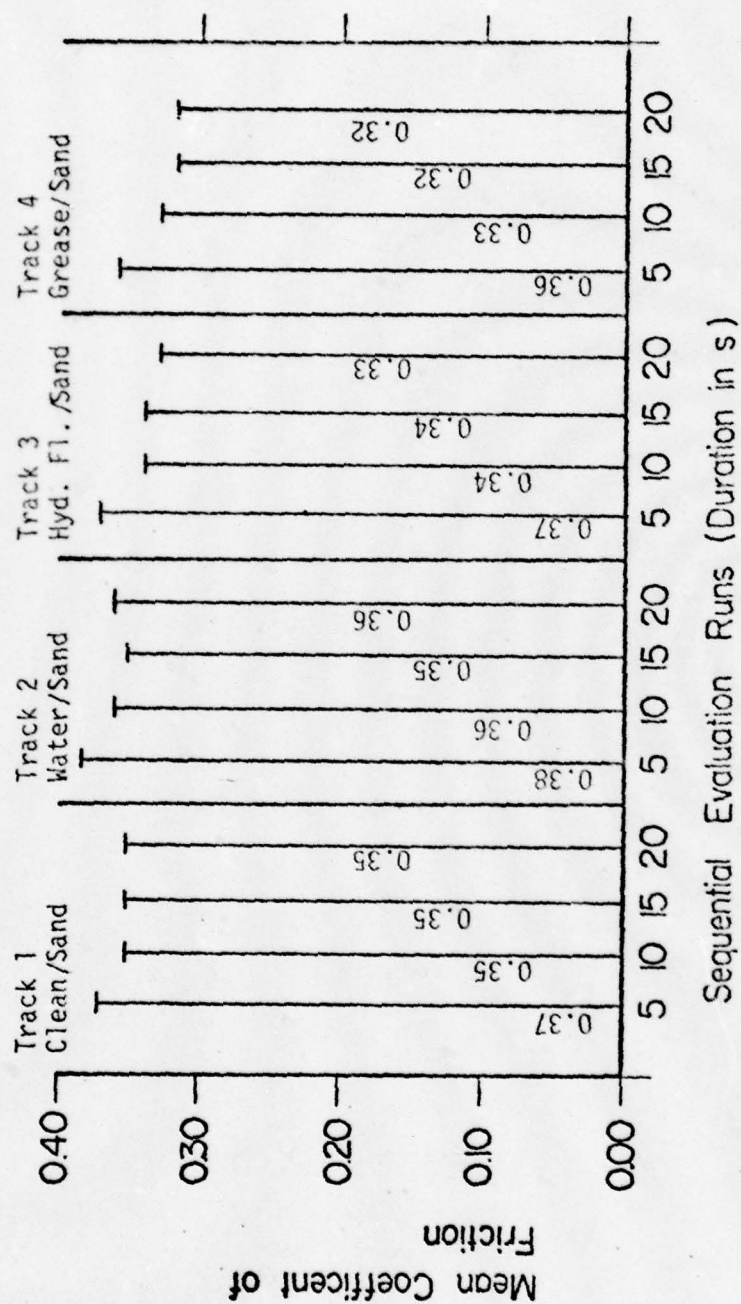
Figure 15 C1 Friction Material on 17-22AS Disc
Standard Liquid Contaminants Followed by
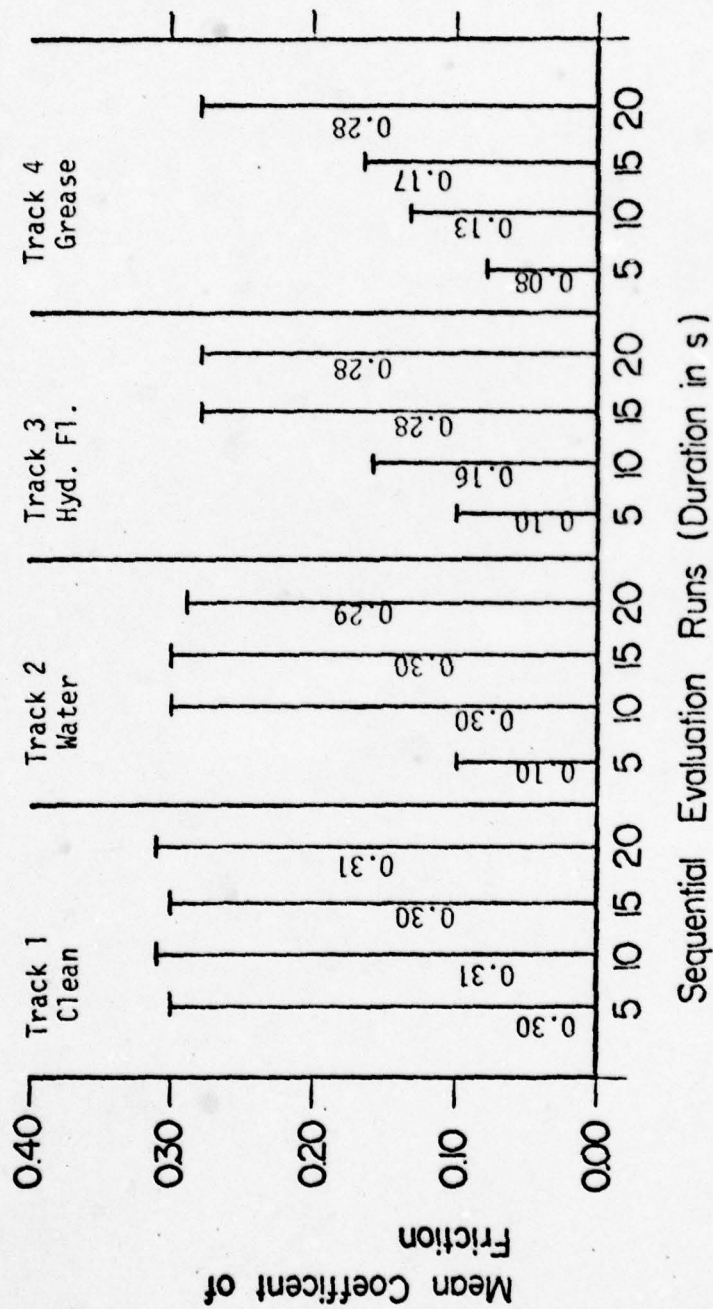Sand Bath and No Recontamination
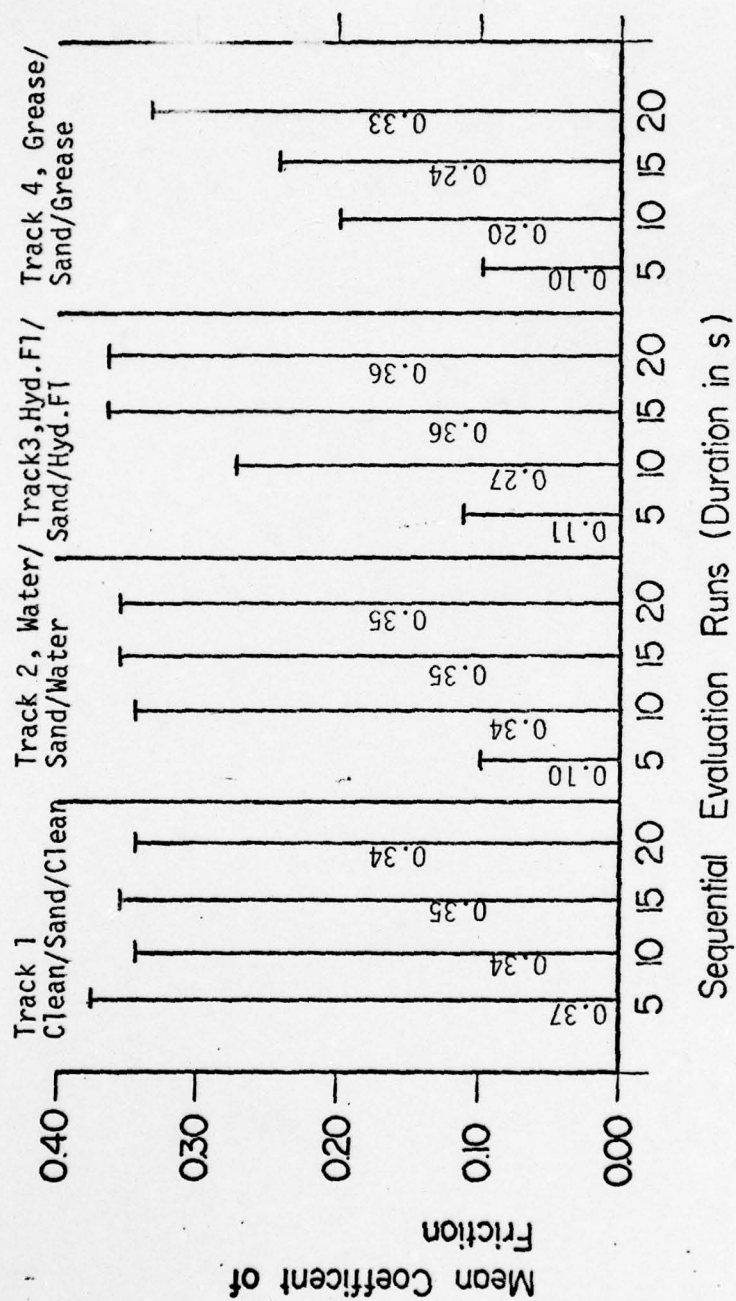
Figure 16   Cl Friction Material on 17-22AS Disc
Standard Liquid Contaminants followed by Sand
Bath and Liquid Recontamination

Approximate Track Smear Area

| Clean | Spot | 20% | 40% | 60% | 80% | Full 0.1 CC Smear |

Runs 123 | Runs 123 | Runs 1234 | Runs 12345 | Runs 123456 | Runs 1234567 | Runs 123456789

Mean Coeff of Friction and Variation

0.40 0.30 0.20 0.10 0.00

Successive Evaluation Runs (5 s Duration Each)
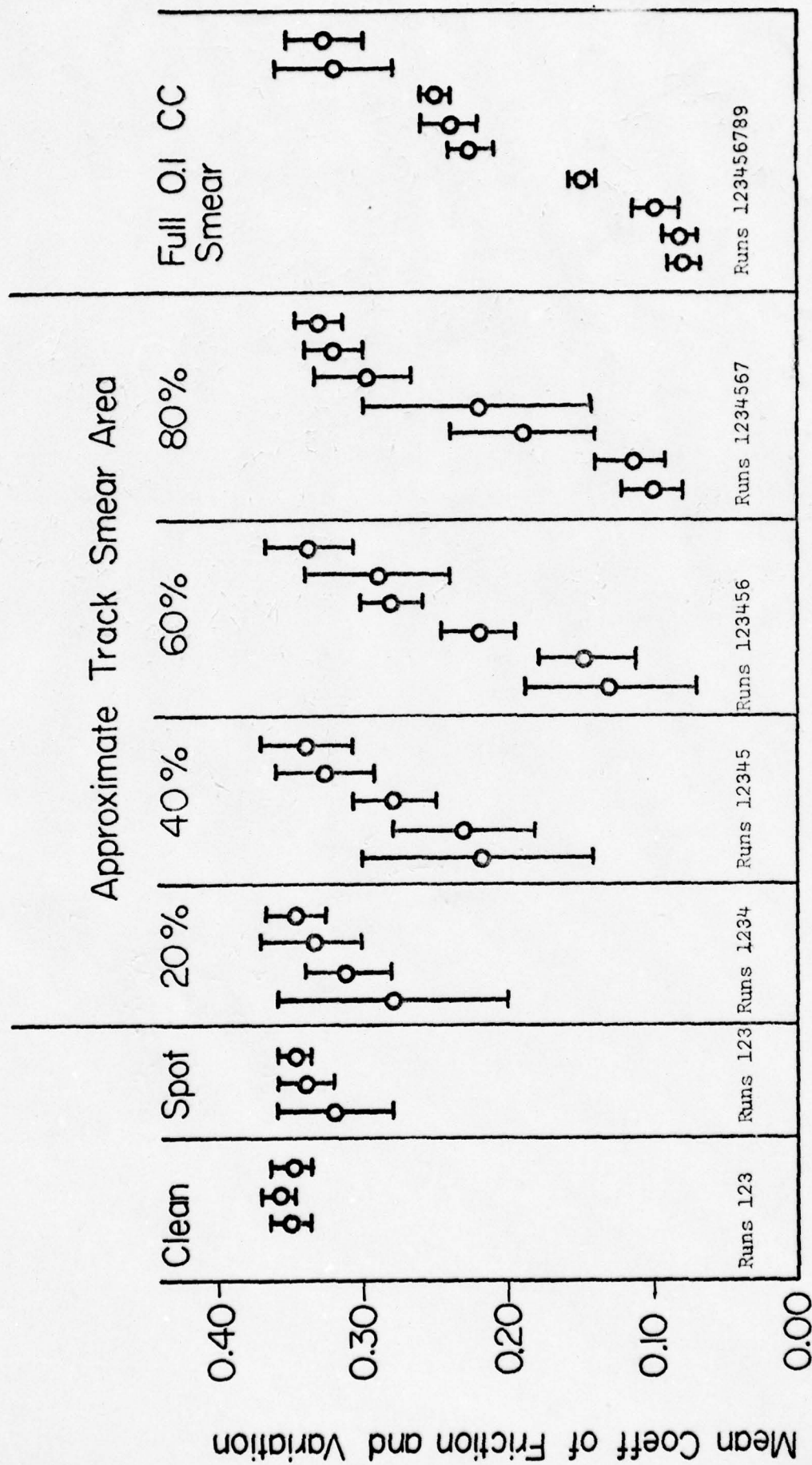
Figure 17   Cl Friction Material on 17-22AS Disc
Grease Contamination Smear Amount Effects
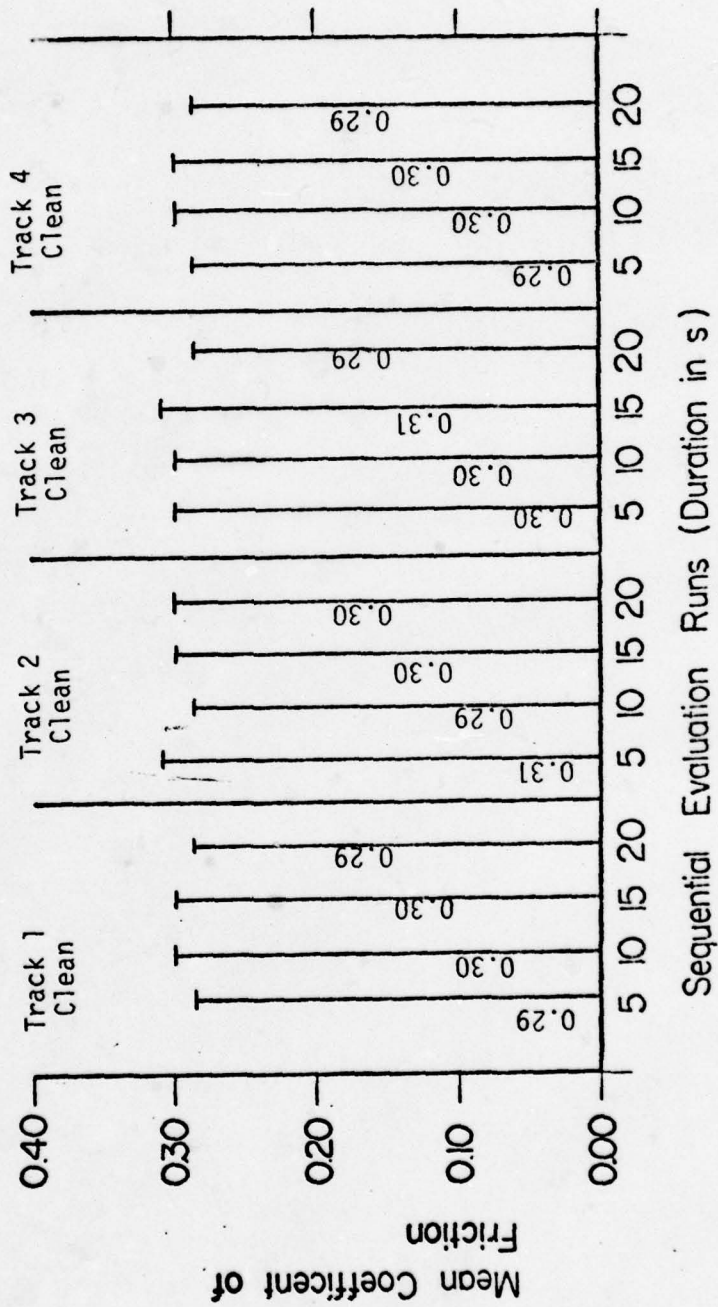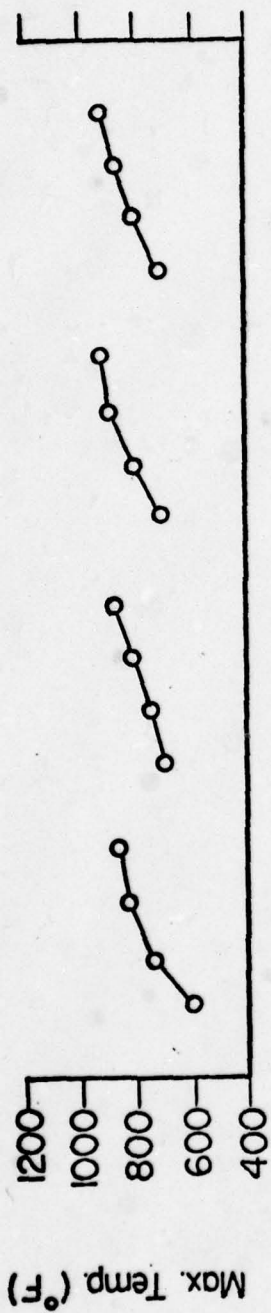
Figure 18 F2 Friction Material on 4140 Hard Disc
No Contaminants

Max. Temp. (°F)

1200 1000 800 600 400

Mean Coefficient of Friction

0.40 0.30 0.20 0.10 0.00

Track 1 Clean   Track 2 Clean   Track 3 Clean   Track 4 Clean

0.29 0.30 0.30 0.29   0.31 0.29 0.29 0.29   0.30 0.28 0.29 0.29   0.28 0.29 0.28 0.27

5 10 15 20   5 10 15 20   5 10 15 20   5 10 15 20

Sequential Evaluation Runs (Duration in s)
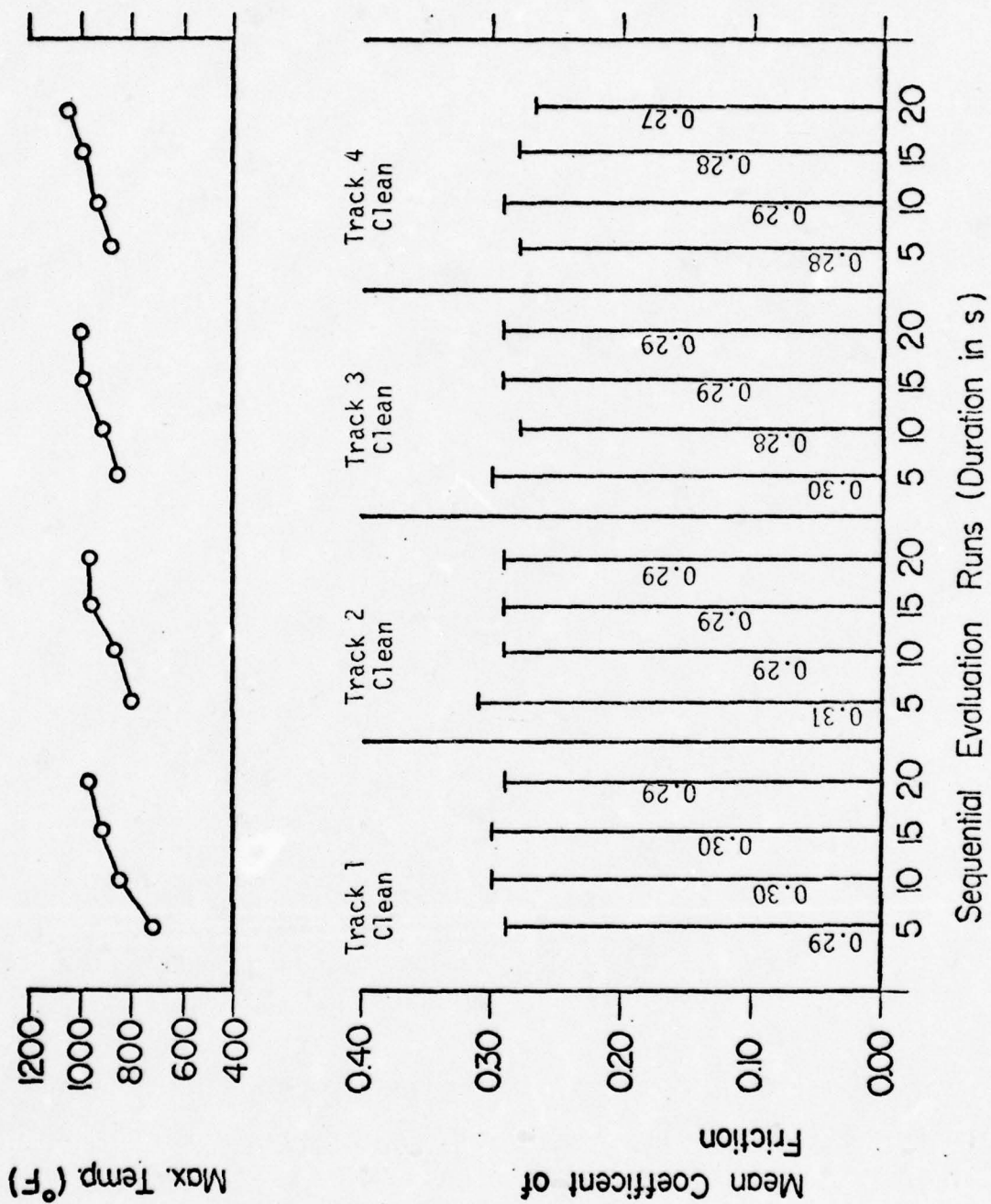
Figure 19   F2 Friction Material on 4140 Hard Disc
No Contaminants with 1 kW Auxiliary Heating
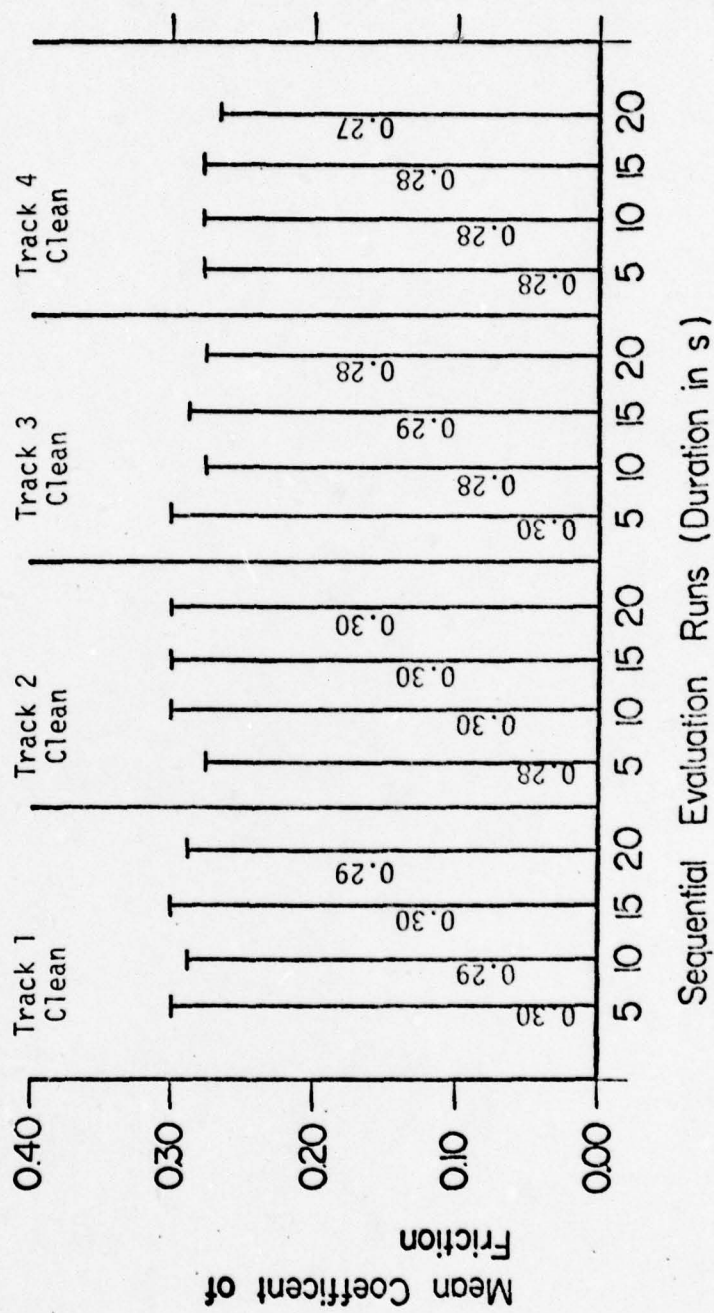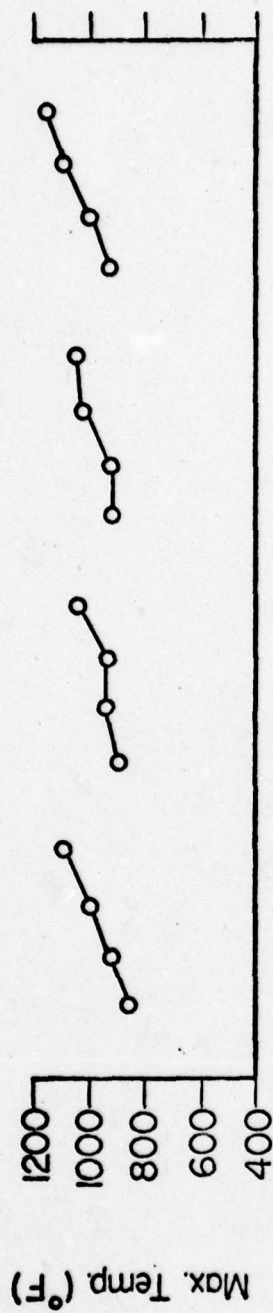
Figure 20 F2 Friction Material on 4140 Hard Disc
No Contaminants with 2 kW Auxiliary Heating
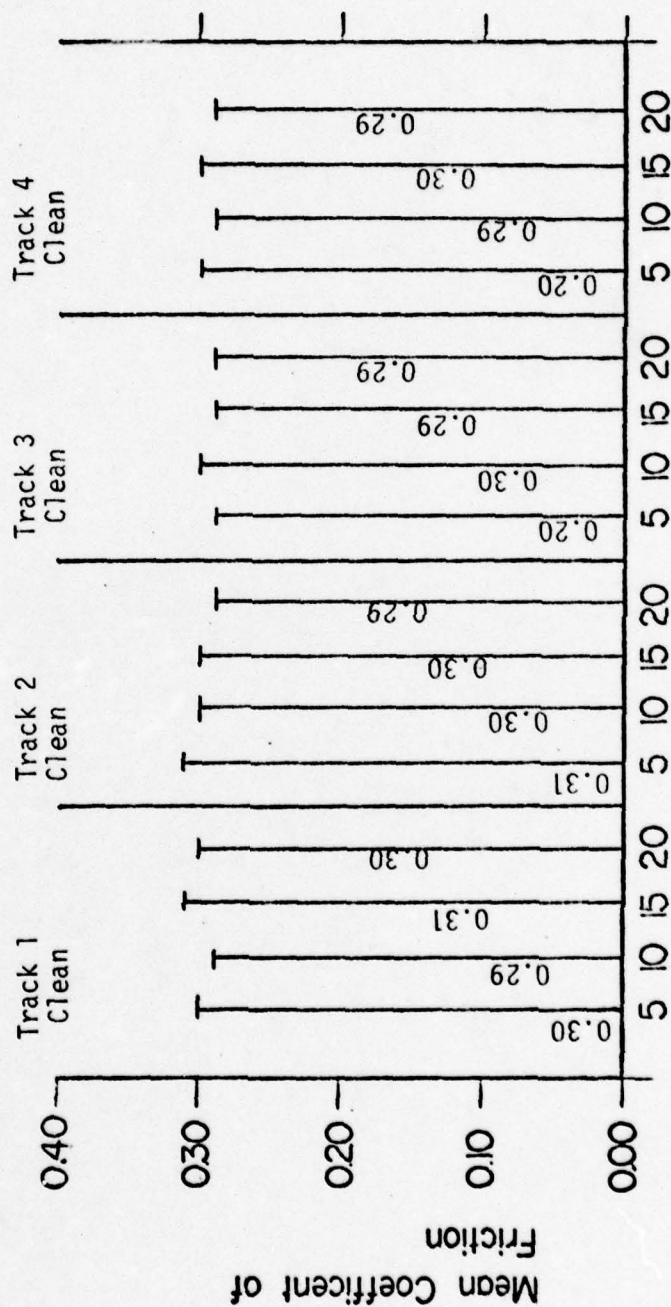
Figure 21 F2 Friction Material on 4140 Hard Disc
No Contaminants at 225 psi Normal Pressure
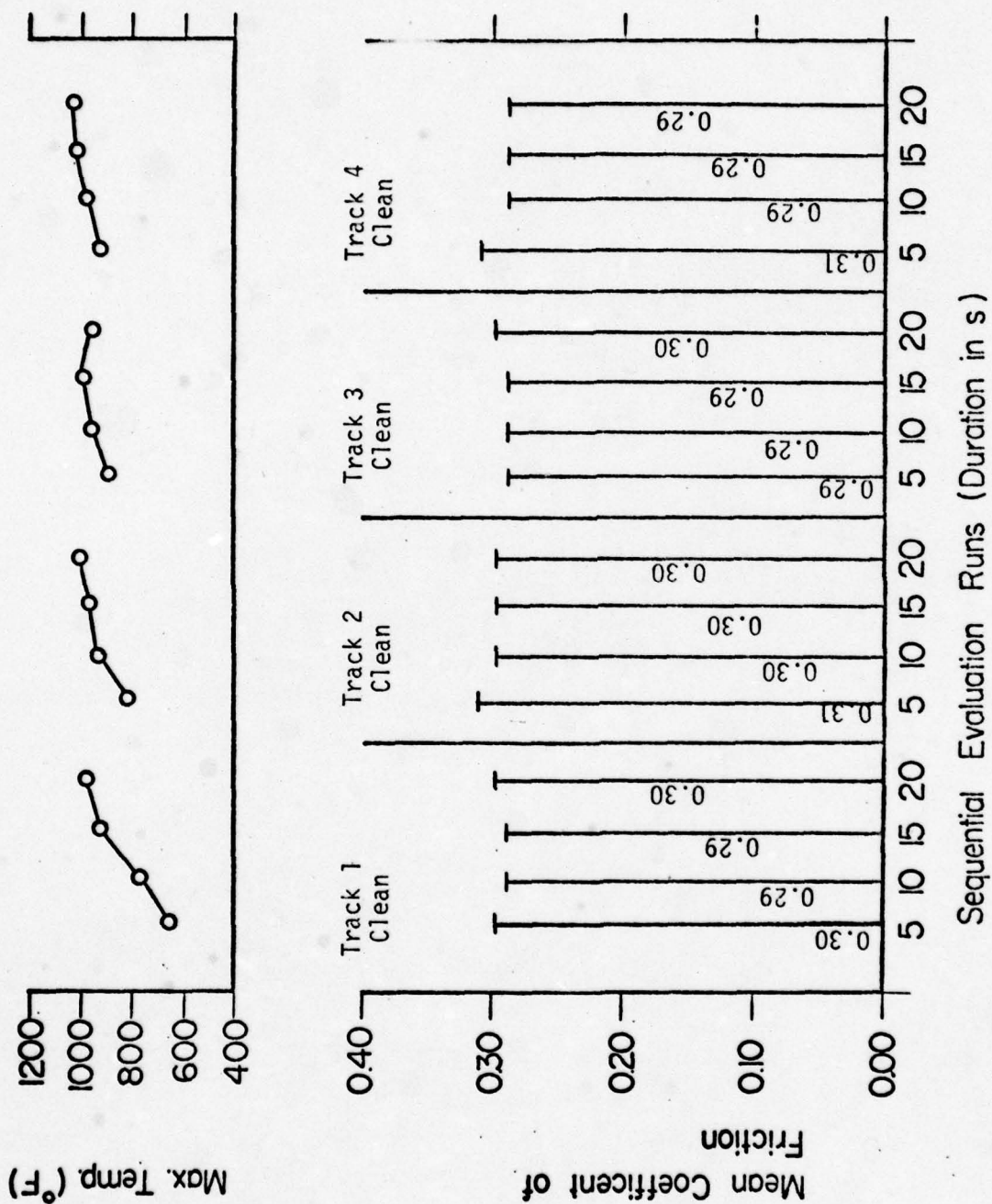
Figure 22 F2 Friction Material on 4140 Hard Disc
No Contaminants and 375 psi Normal Pressure
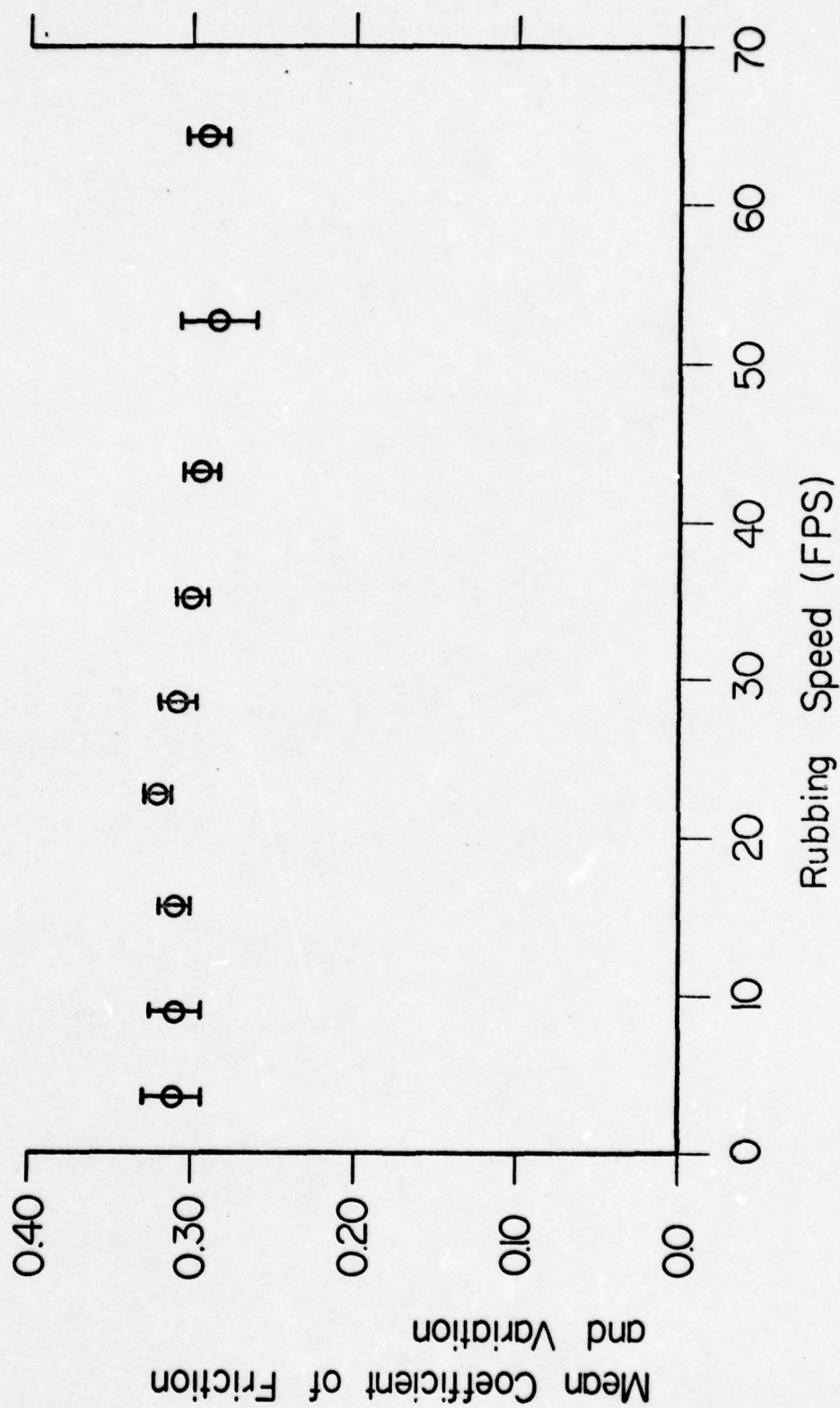
Figure 23 F2 Friction Material on 4140 Hard Disc
No Contaminants, Speed Variation Effects

Table 3 Friction Materials Summary

Material	Density, g/cc	Hardness, Rockwell H Scale	$\bar{\mu}$	Variation/Grab	Fade	Material Transfer	Relative Wear	Physical Observations
C1	4.6	64	0.36	1	1	3	3	Surface Scoring
F1	4.7	76	0.29	1	0	1	2	Minimal Edge Shatter
F2	4.8	73	0.30	1	0	1	1	--
F3	4.7	81	0.30	2	0	2	3	Severe (B) Edge Shatter
N1	4.5	85	0.26	3(A)	1	1	2	Surface Scoring
N2	4.1	40	0.22	3(A)	1	3	3	Surface Scoring
N3	6.7	85	0.25	2(A)	1	1	1	--

0 = none; 1 = minimal; 2 = small; 3 = moderate.

(A) = low speed grab tendencies due to no wear modifiers.

(B) = reduced physical strength due to poor sample sintering.

48

The friction level of the nickel base material was lower than the friction level of the copper and iron materials (0.25 versus 0.35 and 0.30, respectively) and showed more variation and/or grab. It should be noted, however, that the nickel materials tested were in a developmental stage and contained no wear modifiers. Previous researchers [4] have formulated nickel base materials to produce friction levels and minimal variation/grab comparable to the iron base materials tested.

All friction materials demonstrated minimal to no thermal or extended engagement fade.

Due to the screening-type testing methods employed and the corresponding cursory wear observations (visual and simple pad wear volume), wear characterizations of the friction materials tested may be formulated only on a mutually comparative basis as opposed to absolute wear rate. However, supplier information and independent reseachers indicate logistically feasible wear life predictions for properly formulated iron and nickel base friction materials in an FRM application.

All friction materials, except one, demonstrated good physical strength within the load range used. The material with marginal physical characterizations appeared to have been poorly sintered in its as-received configuration. Physically, several friction materials demonstrated gross surface scoring and localized pitting.

The extended friction material tests demonstrated minimal coefficient of friction variations with changes in load, speed, or temperature over the ranges tested. These results typify the performance of many high temperature, wear-optimized sintered metal friction materials.

Various friction contamination simulations demonstrated dramatic friction loss with quick to prolonged recovery of near full uncontaminated friction levels. All contaminant effects and trends appear to be independent of the friction material.

Liquid contaminants (water, hydraulic fluid, and grease) initially drop the coefficient of friction to approximate the 0.1 level or below. Water recovery appears very good although not quickly enough for negligible contaminant effect. Hydraulic fluid and grease recoveries appear similar in a relatively quick recovery to an intermediate level although grease recovery to full friction levels requires a longer period than hydraulic fluid final full recovery.

Grit contamination after liquid contamination raises the normal friction level slightly (0.02 to 0.03) with a recovery speed comparable to that of water. Although infeasible to simulate properly, prolonged grit contamination is expected to have appreciable wear effects primarily on the mating material.

Finally, three important disc material observations were made. (1) Coefficient of friction performance and contaminant effects appear to be independent of the disc materials for the three discs used; (2) While the 17-22AS disc and the 4140 soft disc were not affected appreciably by frictional heating, the hardened 4140 disc had been annealed to Rc 41 from the original Rc 50 over the testing program by frictional heating; and (3) Although increased pad wear could not be correlated to any particular disc, the 4140 soft disc consistently showed visual signs of increased material transfer.

Conclusions--Friction interface contamination will produce catastrophic FRM performance. Foreign media contamination must be prevented. Although contamination recovery is possible, especially for small localized regions, the first recoil pass over the contaminated region will exhibit drastically reduced friction. Vent holes may be drilled transversely in the sliding ways to trap wear debris and grit contamination and to attempt to contain liquid contaminant smear without appreciably adverse effects on the coefficient of friction.

Though nominal disc bulk temperature levels of 900°F were used in testing, rubbing surface temperatures in excess of 1600°F may be experienced [2]. Copper base friction materials are not recommended due to copper softening and smearing at such elevated temperatures. Also, to retain disc surface hardness at these temperatures, 17-22AS steel mating material is recommended.

The life of a friction pad in an FRM is a function of friction material wear characteristics, physical strength, and pad loading methods and forces. The materials tested are only examples of many possible iron or nickel base sintered metal materials which may perform well logistically and physically in conceptualized FRM friction pad loading systems.

Copper and iron base sintered metal friction materials are widely used in industry while nickel base materials are still in various stages of development [1,4]. Based on this fact and the results of this friction material screening program, the F2 friction material is recommended as a preliminary selection for further FRM friction studies and conceptualizations. However, because iron is more susceptible to corrosion than nickel, the status of nickel base friction materials development should be monitored periodically.

It should also be noted that current sintered metal friction materials use graphite as lubricant. Graphite can cause electrolytic corrosion in conjunction with most steels especially in salty environments. However, it is felt that this problem can be chemically and logistically controlled.

Contingent upon FRM feasibility decisions, further friction material studies should be performed: friction interface impulse testing, inertial dynamometry, and final material formulation optimization.

Because an FRM will require prior or immediate friction pad loading on firing, extreme impulse loading at the frictional interface will occur. Friction interface impulse load testing should attempt to check friction material shock transverse shear strength, pad edge shatter, and the effects of impulsive transition from static to sliding coefficient of friction, (see APPENDIX E).

Constant speed drag tests are commonly used for basic friction material screening purposes while inertial dynamometry (brake down to stop of a free rotating inertial mass) is often reserved for more exact material formulation experimentation, prototype simulation, and in-service wear life predictions. Because the constant speed simulated by this study was only a mean predicted recoil speed, inertial dynamometer tests of selected friction materials should be performed using the maximum predicted recoil speed before final prototype design. Although speed effects on these friction materials appear minimal, an inertial dynamometer will better simulate possible high speed wear and transient near stop grab/squeal effects undetectable by constant speed drag testing.

Finally, sintered metal friction materials may be wear optimized for projected thermal and load environments by mixing various modifiers and additives. Recent developmental use of special high temperature additives [4] to augment or replace traditional lubricants and wear modifiers shows considerable promise for high energy FRM applications from wear, fade, and corrosion standpoints.

REFERENCES

1. Bill, R. C., "Some Metal-Graphite and Metal-Ceramic Composites for Use as High-Energy Brake Lining Materials," NASA TN D-7756, Aug. 1974.

2. Ho, T. L., M. B. Peterson, and F. F. Ling, "Effect of Frictional Heating on Brake Materials," Wear, Vol. 30, 1974, pp. 73-91.

3. Ho, T. L., "Some Wear Studies on Aircraft Brake Systems," NASA CR 134989, Oct. 1975.

4. Ho, T. L., and M. B. Peterson, "Development of Aircraft Brake Materials," ASLE 76-LC-1B-3, Oct. 1976.

5. Newcomb, T. P., and R. T. Spurr, Braking of Road Vehicles, Robt. Bentley, Cambridge, Mass., 1969, p. 132.

APPENDIX A: RECOIL SIMULATION EQUATIONS

FRM Friction Force Equations

$$F = I^2/2A + W(\sin \theta - \mu_s \cos \theta)$$

Total Initial Impulse:

$$A = W\ell/g$$

Exact Impulse:

$$A = W\ell/g - H + I t_o$$

Symbol	Units	Definition
F	lb_f	FRM friction force
I	lb_f-s	Breech force impulse (first time integral of breech force curve)
W	lb_f	Weight of recoil mass
g	fps^2	Acceleration of gravity
ℓ	ft	Recoil travel
θ	degrees	Cannon elevation angle
μ_s		Coefficient of friction between recoil and grounded masses
t_o	seconds	Time after firing when breech force nears zero
H	lb_f-s^2	Second time integral of breech force curve through t_o
A	lb_f-s^2	Calculation constant

Sample Calculations

Given values:

	105 Cannon	155 Cannon
$I(lb_f\text{-}s)$	2120	14500
$H(lb_f\text{-}s^2)$	8.81	1290
$t_0(s)$	8.4×10^{-3}	100×10^{-3}
$W(lb_f)$	1500	7000
$\ell(ft)$	2	3

μ_s------------------------0.10

θ(degree)----------------60

FRM friction material
coefficient of friction--0.30

FRM friction material
normal working pressure
(psi)-------------------300

Using Equations:

	105 Cannon		155 Cannon	
	TII	EI	TII	EI
Frictional Force $(10^3 lb_f)$	25.3	23.2	167	135
Normal Force $(10^3 \, lb_f)$	84.3	77.3	557	450
Friction Pad Area $(in.^2)$	281	258	1857	1500

APPENDIX B: COMPUTER RECOIL SIMULATION

An interactive computer routine was used as a design tool to simulate the performance of hypothetical recoil mechansism. The program allowed user definition of various combinations of recoil forces including Coulomb friction, spring compression, and viscous drag.

Computer simulations of recoil force, speed, and energy trends for a 155 mm cannon using three different hypothetical recoil mechanisms are plotted in Fig. Bl. The three simulations shown all incorporated a 275 lb/in. counter-recoil spring and were designed to all produce 3 feet of recoil travel for a 7000 lb recoil mass. The three recoil mechanisms produced recoil forces as shown below:

for x = recoil travel in inches.

v = recoil speed in ft/s,

F = recoil force in lbs,

A - constant load FRM, $F = 112000$

B - recoil spring loaded FRM, $F = 5550 (x + 6)$

C - hypothetical hydro-pneumatic recoil mechanisms
with spring, $F = 114 \ v^2 + 1000(x + 6)$

Tabulations of all user-definable simulation parameters along with a short form simulation output are contained in a sample terminal session printout following Fig. Bl. A FORTRAN source code listing of the program is also included for completeness.
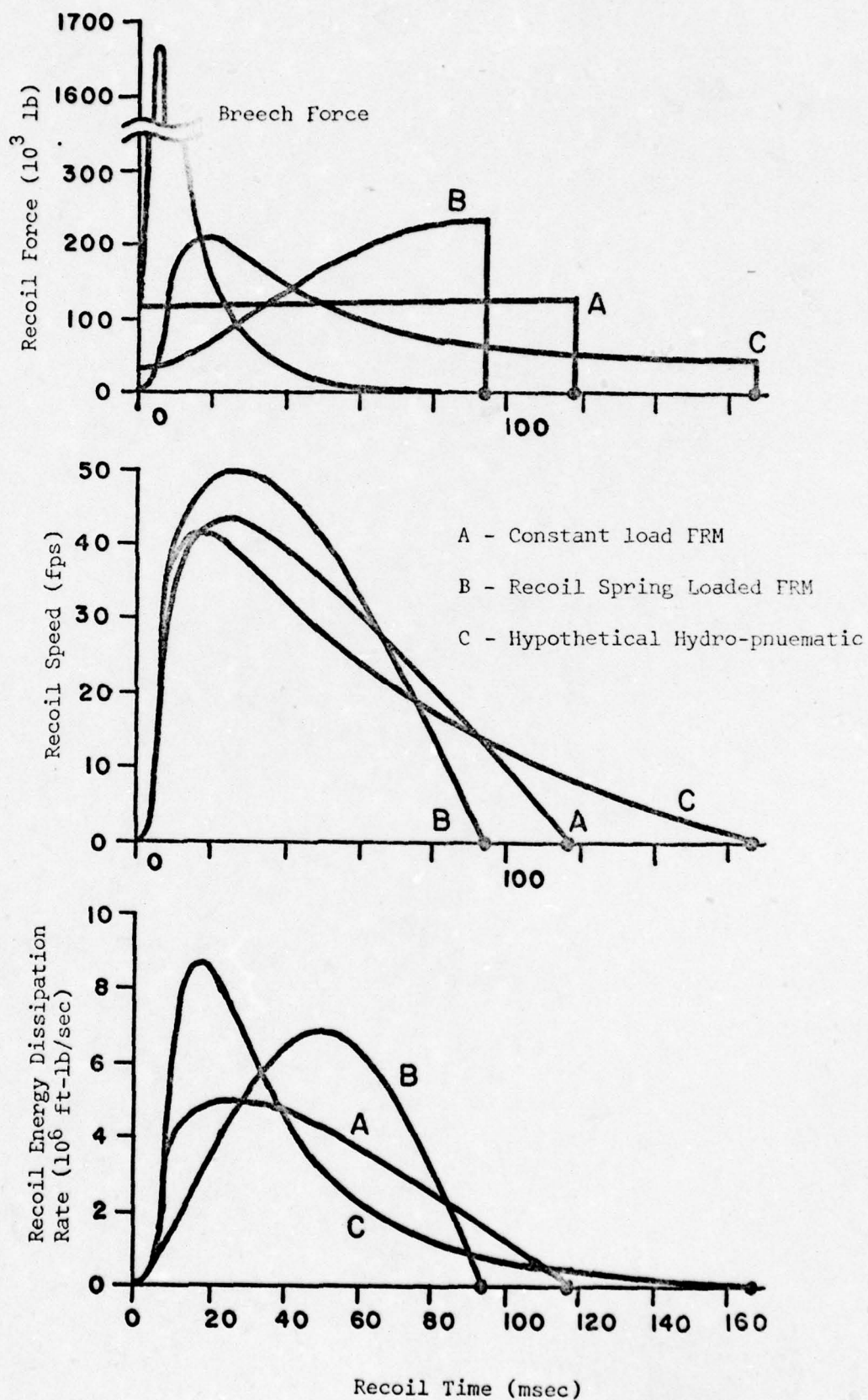
Figure B1   Simulated Performances of 155 mm
Cannon Recoil Mechanisms

SAMPLE TERMINAL SESSION PRINTOUT

```
CANNON RECOIL SIMULATION

SHORT OUTPUT TO TTY ONLY
LONG OUTPUT TO TTY AND FILE RECOIL

155 MM CANNON DEFAULT SET


 STOP=0, RUN=1, LIST=2, CHANGE=3  ? 2

 LIST
 NONE=0, CANNON=1, PROJECTILE=2, RECOIL=3, COUNTER-RECOIL=4  - ALL=5  ? 5

CANNON PARAMETERS
1 - BORE (MM)                                 155
2 - WEIGHT OF RECOIL MASS (LB)            7000.00
3 - ELEVATION ANGLE (DEG)                   60.00
4 - CRADLE FRICTION                           .10

PROJECTILE PARAMETERS
1 - PROJECTILE WEIGHT (LB)                   96.00
2 - IN-TUBE TRAVEL (IN)                     200.00
3 - IN-TUBE DRAG FACTOR                       5.00

RECOIL PARAMETERS
FOR V = RECOIL SPEED
RECOIL FORCE = CONSTANT + C1XV + C2XVXV + C3XVXVXV
1 - CONSTANT (LB)                        112000.00
2 - C1 (LB/FPS)                               0.00
3 - C2 (LB/FPS/FPS)                           0.00
4 - C3 (LB/FPS/FPS/FPS)                       0.00

COUNTER-RECOIL PARAMETERS
1 - SPRING INITIAL DEFLECTION (IN)            6.00
2 - SPRING CONSTANT (LB/IN)                 275.00

 LIST
 NONE=0, CANNON=1, PROJECTILE=2, RECOIL=3, COUNTER-RECOIL=4  - ALL=5  ? 0

 STOP=0, RUN=1, LIST=2, CHANGE=3   ? 3

 CHANGE
 NONE=0, CANNON=1, PROJECTILE=2, RECOIL=3, COUNTER-RECOIL=4 ? 0

 STOP=0, RUN=1, LIST=2, CHANGE=3   ? 1
```

A

```
OUTPUT - SHORT=1, LONG=2 ? 2

END OF RECOIL
TIME (MSEC) =       118.10
TRAVEL (IN) =        36.08
MAX SPEED (FPS) =        43.18                          A

IMPULSE (LB-SEC) =              .1345145E+05
IMPULSE INTEGRAL (LB-SEC-SEC) =          .1435538E+04


STOP=0, RUN=1, LIST=2, CHANGE=3  ? 3

CHANGE
NONE=0, CANNON=1, PROJECTILE=2, RECOIL=3, COUNTER-RECOIL=4 ? 3

CHANGE RECOIL - NONE=0, PARAMETERS=1 THRU 4  ? 1
PARAMETER 1 OLD VALUE 112000.
PARAMETER 1 NEW VALUE  ? 0

CHANGE RECOIL - NONE=0, PARAMETERS=1 THRU 4  ? 3
PARAMETER 3 OLD VALUE 0.
PARAMETER 3 NEW VALUE  ? 114

CHANGE RECOIL - NONE=0, PARAMETERS=1 THRU 4  ? 0

CHANGE
NONE=0, CANNON=1, PROJECTILE=2, RECOIL=3, COUNTER-RECOIL=4 ? 4

CHANGE COUNTER-RECOIL - NONE=0, PARAMETERS=1 OR 2  ? 2
PARAMETER 2 OLD VALUE 275.
PARAMETER 2 NEW VALUE  ? 10000

CHANGE COUNTER-RECOIL - NONE=0, PARAMETERS=1 OR 2  ? 2
PARAMETER 2 OLD VALUE 10000.
PARAMETER 2 NEW VALUE  ? 1000

CHANGE COUNTER-RECOIL - NONE=0, PARAMETERS=1 OR 2  ? 0

CHANGE
NONE=0, CANNON=1, PROJECTILE=2, RECOIL=3, COUNTER-RECOIL=4 ? 0

STOP=0, RUN=1, LIST=2, CHANGE=3  ? 2

LIST
NONE=0, CANNON=1, PROJECTILE=2, RECOIL=3, COUNTER-RECOIL=4  - ALL=5  ? 5
```

```
CANNON PARAMETERS
1 - BORE (MM)                              155
2 - WEIGHT OF RECOIL MASS (LB)         7000.00
3 - ELEVATION ANGLE (DEG)                60.00
4 - CRADLE FRICTION                        .10

PROJECTILE PARAMETERS
1 - PROJECTILE WEIGHT (LB)               96.00
2 - IN-TUBE TRAVEL (IN)                 200.00
3 - IN-TUBE DRAG FACTOR                   5.00

RECOIL PARAMETERS
FOR V = RECOIL SPEED
RECOIL FORCE = CONSTANT + C1XV + C2XVXV + C3XVXVXV
1 - CONSTANT (LB)                         0.00
2 - C1 (LB/FPS)                           0.00
3 - C2 (LB/FPS/FPS)                     114.00
4 - C3 (LB/FPS/FPS/FPS)                   0.00

COUNTER-RECOIL PARAMETERS
1 - SPRING INITIAL DEFLECTION (IN)        6.00
2 - SPRING CONSTANT (LB/IN)            1000.00
```

C

```
 LIST
 NONE=0, CANNON=1, PROJECTILE=2, RECOIL=3, COUNTER-RECOIL=4  - ALL=5  ? 0

 STOP=0, RUN=1, LIST=2, CHANGE=3  ? 1

 OUTPUT - SHORT=1, LONG=2 ? 2

END OF RECOIL
TIME (MSEC) =      167.80
TRAVEL (IN) =       36.00
MAX SPEED (FPS) =      41.69

IMPULSE (LB-SEC) =            .1345145E+05
IMPULSE INTEGRAL (LB-SEC-SEC) =           .2104075E+04
```

C

```
 STOP=0, RUN=1, LIST=2, CHANGE=3  ? 3

 CHANGE
 NONE=0, CANNON=1, PROJECTILE=2, RECOIL=3, COUNTER-RECOIL=4 ? 3

 CHANGE RECOIL - NONE=0, PARAMETERS=1 THRU 4  ? 3
 PARAMETER 3 OLD VALUE 114.
 PARAMETER 3 NEW VALUE  ? 0

 CHANGE RECOIL - NONE=0, PARAMETERS=1 THRU 4  ? 0

 CHANGE
 NONE=0, CANNON=1, PROJECTILE=2, RECOIL=3, COUNTER-RECOIL=4 ? 0

 STOP=0, RUN=1, LIST=2, CHANGE=3  ? 3
```

```
CHANGE
NONE=0, CANNON=1, PROJECTILE=2, RECOIL=3, COUNTER-RECOIL=4 ? 4

CHANGE COUNTER-RECOIL - NONE=0, PARAMETERS=1 OR 2  ? 2
PARAMETER 2 OLD VALUE 1000.
PARAMETER 2 NEW VALUE  ? 5550

CHANGE COUNTER-RECOIL - NONE=0, PARAMETERS=1 OR 2  ? 0

CHANGE
NONE=0, CANNON=1, PROJECTILE=2, RECOIL=3, COUNTER-RECOIL=4 ? 0

STOP=0, RUN=1, LIST=2, CHANGE=3   ? 2

LIST
NONE=0, CANNON=1, PROJECTILE=2, RECOIL=3, COUNTER-RECOIL=4  - ALL=5  ? 5
```

```
CANNON PARAMETERS
1 - BORE (MM)                          155
2 - WEIGHT OF RECOIL MASS (LB)     7000.00
3 - ELEVATION ANGLE (DEG)            60.00
4 - CRADLE FRICTION                    .10

PROJECTILE PARAMETERS
1 - PROJECTILE WEIGHT (LB)           96.00
2 - IN-TUBE TRAVEL (IN)             200.00
3 - IN-TUBE DRAG FACTOR               5.00

RECOIL PARAMETERS
FOR V = RECOIL SPEED
RECOIL FORCE = CONSTANT + C1XV + C2XVXV + C3XVXVXV
1 - CONSTANT (LB)                     0.00
2 - C1 (LB/FPS)                       0.00
3 - C2 (LB/FPS/FPS)                   0.00
4 - C3 (LB/FPS/FPS/FPS)               0.00

COUNTER-RECOIL PARAMETERS
1 - SPRING INITIAL DEFLECTION (IN)    6.00
2 - SPRING CONSTANT (LB/IN)        5550.00
```

B

```
LIST
NONE=0, CANNON=1, PROJECTILE=2, RECOIL=3, COUNTER-RECOIL=4  - ALL=5  ? 0

STOP=0, RUN=1, LIST=2, CHANGE=3   ? 1

OUTPUT - SHORT=1, LONG=2 ? 2
```

```
END OF RECOIL
TIME (MSEC) =        94.20
TRAVEL (IN) =        36.02
MAX SPEED (FPS) =        50.08

IMPULSE (LB-SEC) =              .1345145E+05
IMPULSE INTEGRAL (LB-SEC-SEC) =          .1114048E+04
```

B

FORTRAN SOURCE CODE LISTING

```
        PROGRAM MAIN(INPUT,OUTPUT,RECOIL,TAPE1=OUTPUT,TAPE2=RECOIL)
        REAL CA(4),PR(3),RE(4),CR(2)
        REAL AO(3),AN(3),VO(3),VN(3),S(3)
C
C       INITIALIZE TO 155MM CANNON WITH FRM
C
C       CANNON PARAMETERS
C       IC USED FOR CA(1)
C
        IC=155
        CA(2)=7000.0
        CA(3)=60.0
        CA(4)=0.1
C
C       PROJECTILE PARAMETERS
C
        PR(1)=96.0
        PR(2)=200.0
        PR(3)=5.0
C
C       RECOIL MECHANISM PARAMETERS
C
        RE(1)=112000.0
        RE(2)=0.0
        RE(3)=0.0
        RE(4)=0.0
C
C       COUNTER-RECOIL SPRING PARAMETERS
C
        CR(1)=6.0
        CR(2)=275.0
        PRINT 20000
C
C       CONTROL LOOP
C
10000   CONTINUE
        PRINT *," "
        PRINT *,"STOP=0, RUN=1, LIST=2, CHANGE=3 ",
        READ *,IRUN
        IF(IRUN.EQ.0)GO TO 99999
        IF(IRUN.EQ.1)GO TO 10001
        IF(IRUN.EQ.2)GO TO 10002
        IF(IRUN.EQ.3)GO TO 10002
        GO TO 10000
C
C       LIST/CHANGE LOOP
C
10002   CONTINUE
        PRINT *," "
        IF(IRUN.EQ.2)PRINT *,"LIST"
        IF(IRUN.EQ.3)PRINT *,"CHANGE"
```

```
10015 CONTINUE
      PRINT *,"NONE=0, CANNON=1, PROJECTILE=2,",
      PRINT *,"RECOIL=3, COUNTER-RECOIL=4 ",
      IF(IRUN.EQ.2)PRINT *,"- ALL=5 ",
      READ *,IGR
      IF(IGR.EQ.0)GO TO 10000
      IF(IGR.EQ.5)GO TO 10027
      IF(IGR.LT.1)GO TO 10015
      IF(IGR.GT.4)GO TO 10015
      IF(IRUN.EQ.3)GO TO 10003
C
C     LIST CONTROLLER
C
      GO TO(10004,10005,10006,10007),IGR
10027 CONTINUE
      PRINT 20001,IC,CA(2),CA(3),CA(4)
      PRINT 20002,PR
      PRINT 20003,RE
      PRINT 20004,CR
      GO TO 10002
10004 CONTINUE
      PRINT 20001,IC,CA(2),CA(3),CA(4)
      GO TO 10002
10005 CONTINUE
      PRINT 20002,PR
      GO TO 10002
10006 CONTINUE
      PRINT 20003,RE
      GO TO 10002
10007 CONTINUE
      PRINT 20004,CR
      GO TO 10002
C
C     CHANGE CONTROLLER
C
10003 CONTINUE
      GO TO(10008,10009,10010,10011),IGR
10008 CONTINUE
      PRINT *," "
      PRINT *,"CHANGE CANNON - NONE=0, PARAMETERS=1 THRU 4 ",
      READ *,IP
      IF(IP.EQ.0)GO TO 10002
      IF(IP.EQ.1)GO TO 10012
      IF(IP.LT.2)GO TO 10008
      IF(IP.GT.4)GO TO 10008
      PRINT *,"PARAMETER ",IP," OLD VALUE ",CA(IP)
10013 CONTINUE
      PRINT *,"PARAMETER ",IP," NEW VALUE ",
      READ *,CA(IP)
      IF(CA(IP).LT.0.0)GO TO 10013
      GO TO 10008
```

```
10012 CONTINUE
      PRINT *,"PARAMETER ",IP," OLD VALUE ",IC
10014 CONTINUE
      PRINT *,"PARAMETER ",IP," NEW VALUE ",
      READ *,IC
      IF(IC.EQ.105)GO TO 10008
      IF(IC.EQ.155)GO TO 10008
      GO TO 10014
10009 CONTINUE
      PRINT *," "
      PRINT *,"CHANGE PROJECTILE - NONE=0, PARAMETERS=1 THRU 3 ",
      READ *,IP
      IF(IP.EQ.0)GO TO 10002
      IF(IP.LT.1)GO TO 10009
      IF(IP.GT.3)GO TO 10009
      PRINT *,"PARAMETER ",IP," OLD VALUE ",PR(IP)
10016 CONTINUE
      PRINT *,"PARAMETER ",IP," NEW VALUE ",
      READ *,PR(IP)
      IF(PR(IP).LT.0.0)GO TO 10016
      GO TO 10009
10010 CONTINUE
      PRINT *," "
      PRINT *,"CHANGE RECOIL - NONE=0, PARAMETERS=1 THRU 4 ",
      READ *,IP
      IF(IP.EQ.0)GO TO 10002
      IF(IP.LT.1)GO TO 10010
      IF(IP.GT.4)GO TO 10010
      PRINT *,"PARAMETER ",IP," OLD VALUE ",RE(IP)
10017 CONTINUE
      PRINT *,"PARAMETER ",IP," NEW VALUE ",
      READ *,RE(IP)
      IF(RE(IP).LT.0.0)GO TO 10017
      GO TO 10010
10011 CONTINUE
      PRINT *," "
      PRINT *,"CHANGE COUNTER-RECOIL - NONE=0, PARAMETERS=1 OR 2 ",
      READ *,IP
      IF(IP.EQ.0)GO TO 10002
      IF(IP.LT.1)GO TO 10011
      IF(IP.GT.2)GO TO 10011
      PRINT *,"PARAMETER ",IP," OLD VALUE ",CR(IP)
10018 CONTINUE
      PRINT *,"PARAMETER ",IP," NEW VALUE ",
      READ *,CR(IP)
      IF(CR(IP).LT.0.0)GO TO 10018
      GO TO 10011
```

```
C
C      RUN SEGMENT
C
10001 CONTINUE
      PRINT *," "
      PRINT *,"OUTPUT - SHORT=1, LONG=2 ",
      READ *,IOUT
      IF(IOUT.EQ.1)GO TO 10022
      IF(IOUT.NE.2)GO TO 10001
      WRITE(2,20005)
      WRITE(2,20001)IC,CA(2),CA(3),CA(4)
      WRITE(2,20002)PR
      WRITE(2,20003)RE
      WRITE(2,20004)CR
      WRITE(2,20006)
10022 CONTINUE
C
C      INITIALIZATION OF RUN CONSTANTS AND VARIABLE AT TIME ZERO
C
      THR=CA(3)/57.29577951
      ST=SIN(THR)
      CT=COS(THR)
      CONC=CA(2)*(ST-CA(4)*CT)
      CONP=PR(1)*(ST+PR(3))
      DT=0.0001
C
C      USE EXIT=1.0 FOR PROJECTILE OUTPUT
C
      EXIT=0.0
      VMAX=0.0
      INTER=1
      IF(IC.EQ.155)INTER=10
      DO 10019 I=1,3
      VO(I)=0.0
      S(I)=0.0
10019 CONTINUE
      T=0.0
      CALL BREECH(IC,T,BF)
      RF=RE(1)+CR(2)*CR(1)
      AO(1)=(BF+CONC-RF)*386.088/CA(2)
      AO(2)=(BF-CONP)*386.088/PR(1)
      AO(3)=BF
      F=RF/1000.0
      U=0.0
      IF(IOUT.EQ.2)WRITE(2,20007)T,S(1),VO(1),F,U
C
C      TIME LOOP
C
C      INTEGRATION VARIABLES      A - ACCEL OR BREECH
C                                 V - VEL OR IMPULSE
C                                 S - POS OR INTEGR OF IMPULSE
C                                 N=1  RECOIL MASS
C                                  =2  PROJECTILE
C                                  =3  IMPULSE
C
```

```
                DO 10020 IT=1,30000
                T=FLOAT(IT)*DT
                CALL BREECH(IC,T,BF)
                V=VO(1)/12.0
                RF=RE(1)+RE(2)*V+RE(3)*V*V+RE(4)*V*V*V+CR(2)*(CR(1)+S(1))
                AN(1)=(BF+CDNC-RF)*386.088/CA(2)
                AN(2)=(BF-CDNP)*386.088/PR(1)
                AN(3)=BF
C
C       SIMPSON INTEGRATION AND UPDATE LOOP
C
                DO 10021 I=1,3
                DELTA=DT*(AO(I)+AN(I))/2.0
                IF(VO(I).GT.0.0)GO TO 10025
                IF(DELTA.LT.0.0)DELTA=0.0
10025 CONTINUE
                VN(I)=VO(I)+DELTA
                S(I)=S(I)+DT*(VO(I)+VN(I))/2.0
                AO(I)=AN(I)
                VO(I)=VN(I)
10021 CONTINUE
                TT=T*1000.0
                IF(VO(1).GT.VMAX)VMAX=VO(1)
C
C       LONG OUTPUT PRINT
C
                IF(IOUT.EQ.1)GO TO 10026
                IF(MOD(IT,INTER).NE.0)GO TO 10026
                V=VO(1)/12.0
                F=RF/1000.0
                U=F*V
                WRITE(2,20007)TT,S(1),V,F,U
10026 CONTINUE
C
C       CHECK FOR END OF RECOIL ZERO VELOCITY
C
                IF(VO(1).LT.0.0)GO TO 10023
C
C       CHECK FOR PROJECTILE EXIT
C
                X=(S(1)+S(2))*EXIT
                IF(X.LT.PR(2))GO TO 10020
                EXIT=0.0
                VMUZ=VO(2)/12.0
                WRITE(1,20008)TT,VMUZ
                IF(IOUT.EQ.2)WRITE(2,20008)TT,VMUZ
10020 CONTINUE
C
C       END OF TIME LOOP
C
C       RECOIL END OUTPUT
C
10023 CONTINUE
                VMAX=VMAX/12.0
                WRITE(1,20009)TT,S(1),VMAX,VO(3),S(3)
                IF(IOUT.EQ.2)WRITE(2,20009)TT,S(1),VMAX,VO(3),S(3)
                GO TO 10000
99999 CONTINUE
```

```
C
C     FORMATS
C
20000 FORMAT(/*CANNON RECOIL SIMULATION*/
     1          /*SHORT OUTPUT TO TTY ONLY*
     2          /*LONG OUTPUT TO TTY AND FILE RECOIL*/
     3          /*155 MM CANNON DEFAULT SET*/)
20001 FORMAT(/*CANNON PARAMETERS*
     1          /*1 - BORE (MM)*,T40,I10
     2          /*2 - WEIGHT OF RECOIL MASS (LB)*,T40,F10.2
     3          /*3 - ELEVATION ANGLE (DEG)*,T40,F10.2
     4          /*4 - CRADLE FRICTION*,T40,F10.2)
20002 FORMAT(/*PROJECTILE PARAMETERS*
     1          /*1 - PROJECTILE WEIGHT (LB)*,T40,F10.2
     2          /*2 - IN-TUBE TRAVEL (IN)*,T40,F10.2
     3          /*3 - IN-TUBE DRAG FACTOR*,T40,F10.2)
20003 FORMAT(/*RECOIL PARAMETERS*
     1          /*FOR V = RECOIL SPEED*
     2          /*RECOIL FORCE = CONSTANT + C1XV + C2XVXV + C3XVXVXV*
     3          /*1 - CONSTANT (LB)*,T30,F20.2
     4          /*2 - C1 (LB/FPS)*,T30,F20.2
     5          /*3 - C2 (LB/FPS/FPS)*,T30,F20.2
     6          /*4 - C3 (LB/FPS/FPS/FPS)*,T30,F20.2
20004 FORMAT(/*COUNTER-RECOIL PARAMETERS*
     1          /*1 - SPRING INITIAL DEFLECTION (IN)*,T40,F10.2
     2          /*2 - SPRING CONSTANT (LB/IN)*,T40,F10.2)
20005 FORMAT(/*CANNON RECOIL SIMULATION*)
20006 FORMAT(/*      TIME     TRAVEL      SPEED        RECOIL FORCE*
     1        ,*   ENERGY DISSIPATION*
     2        /*    (MSEC)      (IN)       (FPS)          (1000 LB)*
     3        ,*      (1000 FT-LB/SEC)*/)
20007 FORMAT(3F10.2,2F20.2)
20008 FORMAT(/*PROJECTILE EXIT*
     1          /*TIME (MSEC) = *,F10.2
     2          /*MUZZLE VELOCITY (FPS) = *,F10.2/)
20009 FORMAT(/*END OF RECOIL*
     1          /*TIME (MSEC) = *,F10.2
     2          /*TRAVEL (IN) = *,F10.2
     3          /*MAX SPEED (FPS) = *,F10.2/
     4          /*IMPULSE (LB-SEC) = *,E20.7
     5          /*IMPULSE INTEGRAL (LB-SEC-SEC) = *,E20.7/)
      STOP
      END
```

```
C
C
C      BREECH FORCE CURVES PER RADCON-DOVER
C
C
       SUBROUTINE BREECH(IC,T,F)
       REAL A(91),B(91)
       DATA A/10.,12.,14.,17.,20.,22.,27.,31.,36.,42.,49.,
      1      56.,66.,77.,90.,102.,117.,133.,152.,177.,201.,
      2      228.,254.,285.,321.,353.,390.,420.,451.,479.,508.,
      3      533.,553.,570.,581.,585.,586.,583.,579.,570.,555.,
      4      538.,520.,500.,480.,461.,441.,421.,401.,381.,362.,
      5      343.,325.,308.,293.,277.,261.,248.,236.,224.,211.,
      6      200.,190.,181.,172.,163.,155.,149.,142.,134.,129.,
      7      123.,118.,113.,108.,104.,99.,96.,92.,89.,86.,
      8      82.,79.,76.,74.,71.,68.,65.,62.,60.,59./
       DATA B/9.,17.,38.,69.,136.,167.,151.,116.,94.,66.,54.,
      1      40.,33.,29.,26.,24.,22.,20.,18.,16.5,15.,
      2      14.,13.,12.,11.,10.,9.2,8.5,7.8,7.2,6.8,
      3      6.3,5.9,5.4,5.0,4.6,4.3,4.0,3.7,3.4,3.1,
      4      2.9,2.7,2.5,2.3,2.1,1.9,1.8,1.7,1.6,1.5,
      5      1.5,1.4,1.3,1.2,1.1,1.0,0.9,0.9,0.8,0.8,
      6      0.8,0.8,0.7,0.7,0.7,0.6,0.6,0.6,0.5,0.5,
      7      0.5,0.5,0.5,0.4,0.4,0.4,0.4,0.3,0.3,0.3,
      8      0.3,0.2,0.2,0.2,0.2,0.1,0.1,0.1,0.1,0.1/
       F=0.0
       IF(IC.EQ.155)GO TO 10000
       IT=1+IFIX(T*10000.0+0.0001)
       IF(IT.GT.91)GO TO 99999
       F=1000.0*A(IT)
       GO TO 99999
10000  CONTINUE
       IL=1+(T*1000.0+0.0001)
       IH=IL+1
       IF(IH.GT.91)GO TO 99999
       TL=FLOAT(IL-1)/1000.0
       TH=FLOAT(IH-1)/1000.0
       FL=B(IL)
       FH=B(IH)
       F=FL+(FH-FL)*(T-TL)/(TH-TL)
       F=F*10000.0
99999  CONTINUE
       RETURN
       END
```
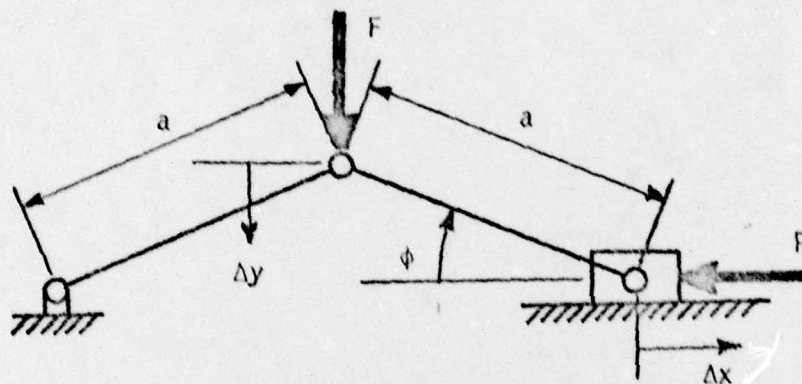
APPENDIX C: FORCE AMPLIFICATION

Toggle Mechanism Equations   .

$$P = F \cot \phi = F(MA)$$

$$\Delta x = 2 \, \Delta y \tan \quad = 2 \, \Delta y(1/MA)$$

Symbol	Units	Definition
a	in.	Toggle arm length
P	lb_f	Output force
F	lb_f	Input actuating force
ϕ	degrees	Toggle angle
Δx	in.	Output travel
Δy	in.	Input travel
MA		Mechanical advantage

Sample Calculations

Given:
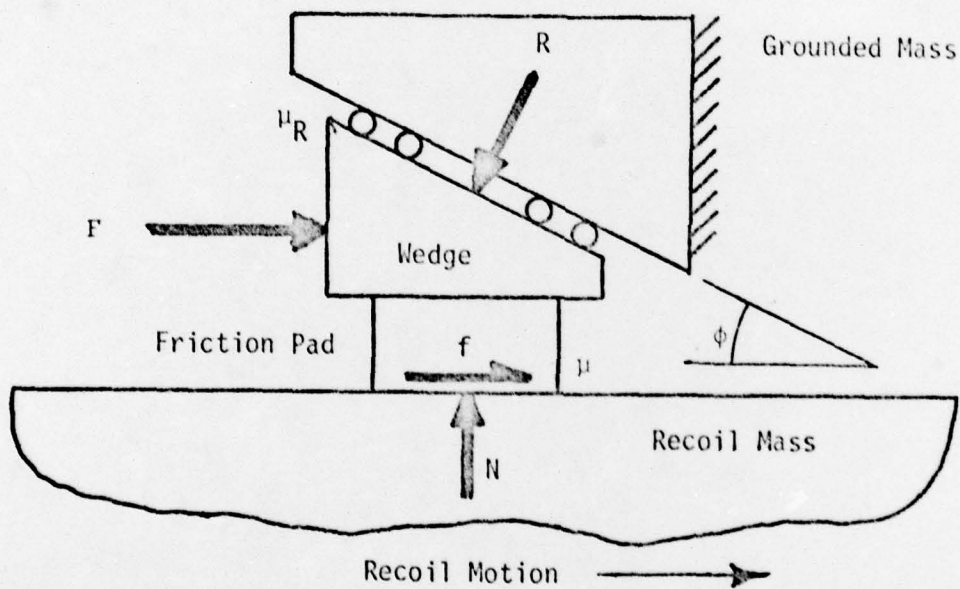
$\phi = 14.5°,$

Using Equations:

$P = 4F,$

$x = 0.5 \Delta y$

Frictional Wedging Self-Energization Equation

$f = \sigma \mu F = \mu N = \mu R(\cos \phi - \mu_R \sin\phi)$

$$\sigma = \frac{\cos \phi - \mu_R \sin \phi}{(1 + \mu \mu_R) \sin \phi - (\mu - \mu_R) \cos \phi}$$

Symbol	Units	Definition
f	lb_f	Frictional force
σ		Self-energization factor
μ		Friction pad coefficient of friction
F	lb_f	Actuating force
N	lb_f	Frictional normal force
R	lb_f	Wedge reaction normal force
ϕ	degree	Wedge angle
μ_R		Wedge coefficient of friction

Sample Calculation

Given values:

$$\mu = 0.30,$$

$$\phi = 25°,$$

$$\mu_R = 0.10,$$

$$f = 17 \times 10^3 \, lb_f \text{ (one of eight pads)}$$

Using Equations:

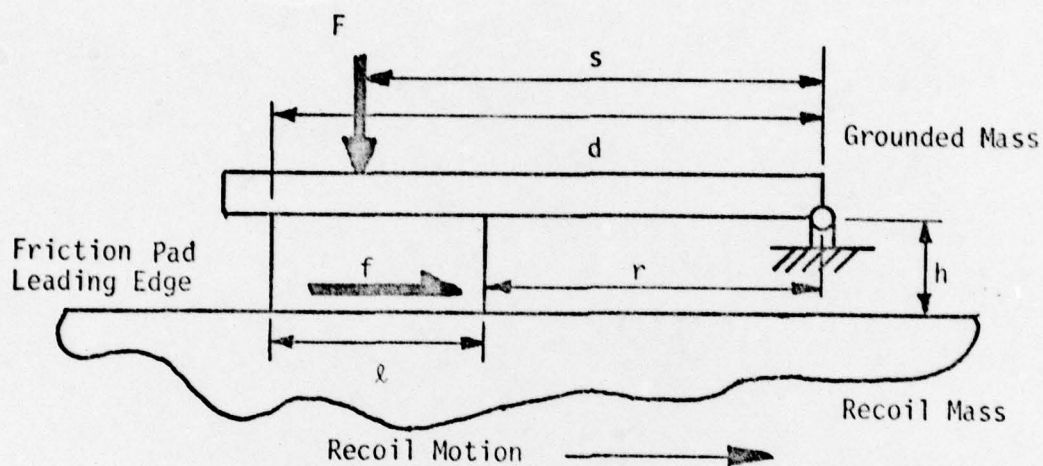$$\sigma = 3.40,$$

$$F = 16.7 \times 10^3 \, lb_f$$

$$N = 56.7 \times 10^3 \, lb_f$$

$$R = 65.6 \times 10^3 \, lb_f$$

Pivoted Pad Self-Energization Equations

$$D = 2(3d^2 - 3\ell d + \ell^2) - 3\mu h(2d - \ell)$$

$$f = \sigma\mu F; \qquad \sigma = 3s(2d - \ell)/D;$$

$$P_{max} = \rho(F/\ell w); \qquad \rho = 6sd/D;$$

$$f = \psi\,\mu p_{max}\,d^2; \qquad \psi = (2d - \ell)\ell w/2d^3$$

Symbol	Units	Definition
d	ft	Pad leading edge to pivot distance
ℓ	ft	Pad length
μ		Pad coefficient of friction
h	ft	Pivot height above friction surface
s	ft	Load application distance from pivot
W	ft	Pad width
f	lb_f	Frictional force
σ		Self-energizing factor
F	lb_f	Actuating foce
P_{max}	psi	maximum pad normal pressure
ρ		Pressure factor
ψ		Width factor
D	ft^2	Calculation constant

NOTE: To prevent pad trailing edge shatter by localized locking use

$r > \mu h$.

Using Dimensionless Parameters

$$\alpha = s/d; \quad \beta = \ell/d; \quad \delta = h/d; \quad \delta = w/d;$$

$$E = 2(3 - 3\beta + \beta^2) - 3\mu\delta(2 - \beta)$$

$$= 3\alpha(2 - \beta)/E; \quad \rho = 6\alpha/E; \quad \phi = 0.5(2 - \beta)\beta\delta$$

Sample Calculations

Given values:

$d = 3$ ft

$s = 3$ ft $\alpha = 1$

$\ell = 2.7$ ft $\beta = 0.9$

$h = 1.2$ ft $\delta = 0.4$

$\mu = 0.3$

$f = 17 \times 10^3$ lb$_f$ (one of eight pads)

$P_{max} = 300$ psi

Using equations:

$\sigma = 1.81$ $F = 31.3 \times 10^3$ lb$_f$

$\rho = 3.29$ $\omega = 10.6$ in.

$\phi = 0.146$

$\delta = 0.294$

APPENDIX D COUNTER-RECOIL SPRING

Counter-recoil Spring Equation

$$k = \frac{W[2\ell \sin \theta + 2\mu_s \ell \cos \theta + (v^2/g)]}{\ell(2x_o + \ell)}$$

Symbol	Units	Definition
k	lb_f/ft	Counter recoil spring constant
W	lb_f	Weight of recoil mass
g	fps^2	Acceleration of gravity
ℓ	ft	Recoil travel
θ	degrees	Cannon elevation angle
μ_s		Coefficient of friction between recoil and grounded masses
v	fps	Recoil mass velocity at end of counter recoil
x_o	ft	Initial deflection of spring

<u>Sample Calculations</u>

Given values:

	105 Cannon	155 Cannon
$W(lb_f)$	1500	7000
$\ell(ft)$	2	3
μ_s		0.1
$v(fps)$		0
$x_o(ft)$		0.5
$\theta(degees)$		60

Using Spring Equation:

	105 Cannon	155 Cannon
$k(lb_f/ft)$	912	3204
$k(lb_f/in.)$	76	267

Sample Helical Compression Spring with Squared and Ground Ends:

Outside Diameter--------------------15

Inside Diameter--------------------12

Wire Diameter----------------------1.5

Free Height------------------------60 in.

Compressed Height------------------18.45

Number of Coils--------------------12.3

Number of Active Coils------------10.3

Spring Constant-------------------262 lb_f/in.

APPENDIX E: FRICTION MATERIAL IMPULSE SHEAR TESTING

Proposed FRM frictional braking using sintered metal friction materials differs from current uses of these materials in two ways. The duration of brake actuation on aircraft and off-road vehicles is on the order of 20 seconds while FRM braking stop time will be on the order of 100 milliseconds. Also, current sintered metal braking applications load the friction pad onto a kinetic friction surface while FRM conceptualizations will preload the friction pad onto a stationary friction surface which will become kinetic by the impulse of firing.

Both of the above differences will produce large impact-like shearing stresses in the friction material at and near the friction interface. The physical and frictional performance of sintered metal materials subjected to such impulsive shear loading has never been simulated and has direct bearing on FRM feasibility considerations.

Two possible impact shear testing methods for candidate friction materials may be used. The first would use an existing full-size impact powder recoil gymnasticater to supply the basic hardware and impulse generation. For simplicity of hardware modification, friction sliding ways would be attached to the grounded mass and hydraulic calipers with flexible supply lines would be attached to the recoiling mass to load full-size sample pads of the friction material onto the sliding ways.

An alternative impact shear testing method would be to use a scaled rig to test small friction material samples. The dead-blow of a pendular weight on a small recoiling mass would provide a scaled impulse. Scaled friction ways and hydraulic caliper loading of the friction material specimen would be required to reproduce the nominal rubbing speeds, friction material normal pressure, and stop time predicted for full-size FRM operation.